

An Extended Rotary Energy Harvester Using Multiple Piezoelectric Cantilevers

DU, Xiaona

A Thesis Submitted in Partial Fulfillment
of the Requirements for the Degree of
Master of Philosophy

in

Mechanical and Automation Engineering
The Chinese University of Hong Kong

June 2011



Thesis/ Assessment Committee

Professor Wei-Hsin Liao (Thesis Supervisor)

Professor Wen-Jung Li (Chair)

Professor Ruxu Du (Committee Member)

Professor Wen-Jong Wu (External Examiner)

ABSTRACT

During the last decade, the technique of piezoelectric energy harvesting (PEH) has been widely investigated to scavenge energy from ambient vibrations or movements. Piezoelectric energy harvesters could replace batteries to serve as the power supply for wireless sensor networks with low power consumption. Researches were carried out for the energy harvesting from floors and roads. Rotary movements are also widespread so that they can be the energy source for PEH as well. In this thesis, a new energy harvesting device is designed to scavenge energy from rotary devices, which can be utilized in windmills, rotary entrance gates, and ticket gates in metro stations and supermarkets. The harvester consists of piezoelectric elements loaded in cantilever beams and a rotary cylinder with plectra distributed in a particular arrangement on the cylindrical surface. Torque is applied through the rotary motion to drive the cylinder to rotate. Then the plectra will transmit the torque seriatim to the cantilevers. This extended distribution of the plectra on the cylinder surface will in turn apply force on each of the cantilevers. An analytical model is developed and analysis of this device is performed. Prototype is fabricated and tested to validate the proposed idea, and the power performances of the extended rotary energy harvester (E-REH) are evaluated and compared with the original rotary energy harvester. The working range of the E-REH is also discussed.

摘要

近十年來，壓電能量收集技術正被廣泛地研究與開發利用。壓電元件基於正壓電效應，可以將周圍的振動或者移動轉化成電能儲存並加以利用。地鐵和火車站巨大的客流量使得檢票口成為一個潛在的能量來源，尤其是在香港這樣的國際大都市，客流量更加可觀。本文提出了一個可裝載於地鐵閘門上的延伸式旋轉能量收集器。它由一組壓電懸臂梁和一個帶有齒的可旋轉的圓柱體組成。這個旋轉圓柱體上均勻的分佈著一組或幾組齒，這些齒的分佈是延伸階梯式排布，這使得一組平行排列的壓電梁可分別被對應的齒先後撥動，因此，由旋轉運動產生的力矩可作用於對應的一根壓電懸臂梁。這種分佈構成的裝置對使用者產生的阻力相對可以降低很多。另外，本論文還提出一個基於衝擊力的用於壓電振動系統的分析模型。此模型可用於分析預測這一特定結構中壓電懸臂梁的振動行為和裝置的能量輸出。本論文對加工的原型進行了測試，對其能量輸出進行了檢驗和評估，並對分析模型進行驗證。最後本論文通過這一延伸式旋轉能量收集器與普通旋轉式能量收集裝置的性能對比分析，對這一新型結構適用範圍及可能的應用進行了討論。

ACKNOWLEDGEMENTS

I would like to give my hearty appreciation to my thesis supervisor, Professor Wei-Hsin Liao (廖維新教授), whose encouragement, guidance and support from the initial to the final stages enabled me to develop this research. I am also very grateful to Professor Ruxu Du (杜如虛教授), Professor Wen-Jung Li (李文榮教授), and Professor Wen-Jong Wu (吳文中教授) for serving as my committee members and providing comments on this research.

I would like to express my appreciation to my parents Mr. Du Huixiang and Ms. Yang Guijuan (杜惠祥先生, 楊桂娟女士) – for their love and support, to SMS Lab members – Dr. Chan Kwong Wah (陳光華博士), Dr. Chen Jinzhou (陳金舟博士), Dr. Dr. Liang Junrui (梁俊睿博士), Dr. Guo Hongtao (郭洪濤博士), Dr. Liu Lu (劉璐博士), Dr. Shen Chien Yu (沈建佑博士), Dr. Pan Chengliang (潘成亮博士), Miss. Jia Jiangying (賈江瑩小姐), Mr. Chen Chao (陳超先生), Mr. Cheung Ming Fai (張明輝先生) and Mr. Chan Chi Chong (陳始創先生) – for the discussions and their help in experiments and the friendship in daily life.

TABLE OF CONTENTS

ABSTRACT.....	i
摘要	ii
ACKNOWLEDGEMENTS	iii
TABLE OF CONTENTS	iv
LIST OF FIGURES.....	vi
LIST OF TABLES	ix
CHAPTER ONE INTRODUCTION	1
1.1 Background	2
1.1.1 Development of portable devices	2
1.1.2 Energy harvesting	2
1.1.3 Piezoelectric energy harvesting	5
1.1.4 Impact based piezoelectric energy harvester	10
1.1.5 Operation of piezoelectric materials	14
1.2 Research Objective	16
1.3 Thesis Organization	19
CHAPTER TWO DESIGN AND MODELING OF AN EXTENDED ROTARY ENERGY HARVESTER	20
2.1 Design Considerations of an Extended Rotary Energy Harvester	20
2.2 Models of Rotary Energy Harvesters.....	24
2.3 Simulation Results	33
2.4 Chapter Summary	37
CHAPTER THREE PROTOTYPE, TESTING AND OUTPUT POWER OF EXTENDED ROTARY ENERGY HARVESTER	38

3.1 Prototype and Experiment..... 38

3.2 Output Power..... 44

 3.2.1 Maximum tip displacement on output power 44

 3.2.2 Rotational frequency on output power 47

3.3 Chapter Summary 50

CHAPTER FOUR COMPARISON BETWEEN E-REH AND REH 51

4.1 Force on Output Power 52

4.2 Rotational Frequency on Output Power..... 54

4.3 Comparison on Design Space..... 59

4.4 Chapter Summary 62

CHAPTER FIVE CONCLUSION AND FUTURE WORK 63

5.1 Conclusion..... 63

5.2 Future Work 64

BIBLIOGRAPHY 65

LIST OF FIGURES

Figure 1.1-1 Comparison of various alternatives for power sources (Priya, 2007)	4
Figure 1.1-2 Schematic and picture of fabricated prototype “Piezoelectric Windmill” (Priya et al., 2005)	9
Figure 1.1-3 Conceptual representation of the impact-based vibration energy harvester (Renaud et al., 2009).....	12
Figure 1.1-4 Schematic illustration of the piezoelectric direction of forces applied and voltage generated in two operation modes (a) d33 mode; (b) d31 mode	14
Figure 1.2-1 Potential energy sources for rotary energy harvesting.	17
Figure 2.1-1 Schematic design of the rotary energy harvester (REH)	21
Figure 2.1-2 Schematic design of the extended rotary energy harvester (E-REH).....	22
Figure 2.2-1 Four general impact problems: (a) particle impact (stereo-mechanical), (b) rigid body impact, (c) transverse deformations of flexible bodies, and (d) axial deformation of flexible bodies (Stronge, 2000).	25
Figure 2.2-2 Equivalent model of a vibrating structure with bonded piezoelectric elements (Badel et al., 2005).....	27
Figure 2.2-3 Equivalent circuit of PEH device	30
Figure 2.2-4 Impedance properties measured by impedance analyzer	31
Figure 2.2-5 Simulink model for impact based rotary energy harvester	32
Figure 2.3-1 Time response of the output voltage (1 Hz rotational frequency, $u_{max} =$ 0.7 mm)	34
Figure 2.3-2 Time response of the output voltage (2 Hz rotational frequency, $u_{max} =$ 1.4 mm)	34
Figure 2.3-3 Output power versus maximum tip displacement ($f = 0.78$ Hz)	35

Figure 2.3-4 Output power versus rotational frequency ($u_{max} = 1.5 \text{ mm}$)	36
Figure 3.1-4 QuickPack piezoelectric bimorph cantilever (QP21 from MIDE Company).....	41
Figure 3.1-5 Schematic diagram of the experimental setup	43
Figure 3.2-1 Schematic of the impact process	45
Figure 3.2-2 Time response of output voltage ($f = 1 \text{ Hz}$, $u_{max} = 1.5 \text{ mm}$)	45
Figure 3.2-3 Output power versus maximum tip displacement ($f = 0.78 \text{ Hz}$)	46
Figure 3.2-4 Average output power versus rotational frequency ($u_{max} = 1.5 \text{ mm}$)	47
Figure 3.2-5 Average power output versus load resistance ($u_{max} = 1.5 \text{ mm}$, $f = 1.25 \text{ Hz}$)	49
Figure 4.1-1 Power output comparison between E-REH and REH under input pulse with varying force amplitude ($f = 1 \text{ Hz}$)	52
Figure 4.1-2 Critical force versus total stiffness and maximum tip displacement.....	53
Figure 4.2-1 Time response of output voltage by one piezoelectric cantilever in REH ($f = 0.2 \text{ Hz}$)	54
Figure 4.2-2 Time response of output voltage by one piezoelectric cantilever in REH ($f = 1 \text{ Hz}$)	55
Figure 4.2-3 Time response of output voltage by one piezoelectric cantilever in REH ($f = 10 \text{ Hz}$)	55
Figure 4.2-4 Time response of output voltage by one piezoelectric cantilever in REH ($f = 13 \text{ Hz}$)	56
Figure 4.2-5 Comparison on output power between E-REH and REH with varying rotational frequency	58
Figure 4.3-1 Variation of the output power by E-REH under different impact force and rotational frequency	59

Figure 4.3-2 Variation of the output power by REH under different impact force and rotational frequency60

Figure 4.3-3 Variations of the output power by both E-REH and REH under different impact force and rotational frequency60

LIST OF TABLES

Table 2.2-1 Definitions of piezoelectric material properties	28
Table 2.2-2 Definitions of parameters and constants	31
Table 2.3-1 Parameter values.....	33
Table 3.1-1 Piezoelectric constants of the ceramics (CTS-3195HD)	43
Table 3.2-1 Parameters in equivalent circuit	49

CHAPTER ONE INTRODUCTION

This chapter presents background knowledge and related literature reviews on energy harvesting, especially piezoelectric energy harvesting and related devices. Design and applications for these devices are described. Basic knowledge and general information about piezoelectric materials are introduced. At the end of this chapter, the research objective and organization of this thesis are introduced.

1.1 Background

1.1.1 Development of portable devices

Wireless sensor networks (WSNs) have been fast developed. The power supply for these electronics is usually conventional batteries. It could be troublesome to replace batteries. If ambient energy can be transferred into electrical energy to power the WSNs, this problem could be resolved. Therefore, the research area of energy harvesting has experienced significant growth and development over the past few years due to the increasing demand by portable and wireless electronics (Cook-Chennault et al., 2008). Thus, the demand of energy harvesting and self-powered technologies is increasing fast. The energy around the device such as wasted heat, vibration, wind and solar energy as well as RF radiation could be the energy source for the energy harvesting and scavenging (Mateu and Moll, 2005; Hudak and Amatuucci, 2008).

1.1.2 Energy harvesting

Energy harvesting is the technology by which energy is extracted from ambient energy sources, e.g., solar power (Regan and Gratzel, 1991), thermal energy (Kyono et al., 2003), wind energy (Ackermann and Soder, 2000), and kinetic or gravitational potential energy (Roundy et al., 2003). The extracted energy can then be converted into electricity and stored. Energy harvesting devices include windmills, solar panels, and so on. They collect the energy that exists in nature, such as wind energy and solar

energy. The research on energy harvesting is multidisciplinary. Investigations have been conducted by researchers from diverse disciplines.

Xie et al. (2009) have proposed an automatic winding device of mechanical watch movement and its application in energy harvesting. It utilized a pendulum mechanism with a set of gears to convert the bidirectional motion into unidirectional motion for harvesting the kinematical energy from human motions. The simulation results showed that the efficiency of the device is about 46.3% and it could be used as power supply for various mobile electronic devices with further optimizations.

The term “Energy Harvesting” is frequently used when talking about small, wireless autonomous devices, like those used in wearable electronics and wireless sensor networks (Wikipedia http://en.wikipedia.org/wiki/Energy_harvesting). Numerous researches were previously reported on micro power generators that use different conversion mechanisms, for examples, electromagnetic (Kulah and Najafi, 2004), electrochemical (Milliken et al., 1999), thermoelectric (Leurial et al., 2001), thermophotovoltaic (Yang et al., 2003), photovoltaic (Sakakibara et al., 2002), and piezoelectric (Fang et al., 2006). One driving force behind the search for new energy harvesting devices is the desire to provide the possibility that someday the ICs and sensor nodes can be self-powered and endure a longer lifetime. Yuen et al. (2007) have proposed an AA-sized micro power generator that could power the off-the-shelf ICs by converting vibration into electricity. Together with a start-up circuit and a voltage regulator, this micro power generator could power a wireless thermometer that had an average power consumption of 27.6 mW.

Wireless sensor networks (Gilbert and Balouchi, 2008; Mathuna et al., 2008; Bogue, 2009; Op het Veld et al., 2009), and portable electronics (Paradiso and Starner, 2005; Jia and Liu, 2009) are the most potential beneficiaries of energy harvesting technologies. Figure 1.1-1 shows the comparison of various alternative energy sources for energy harvesting (Priya, 2007).

Solar energy generation has been developed over the years. But one of the main limitations for solar energy generation is that the power density is relatively low inside the building (Priya, 2007). The other most attractive energy source is mechanical energy that exists in vibrations, air flow, and human power. The mechanical energy can be harvested by piezoelectric, electromagnetic or electrostatic mechanisms. The author also pointed out that piezoelectric transducers are more suitable for the energy conversion from kinetic to electrical with the advantages of smaller, lighter and three times higher energy density as compared to other two methods: electrostatic and electromagnetics.

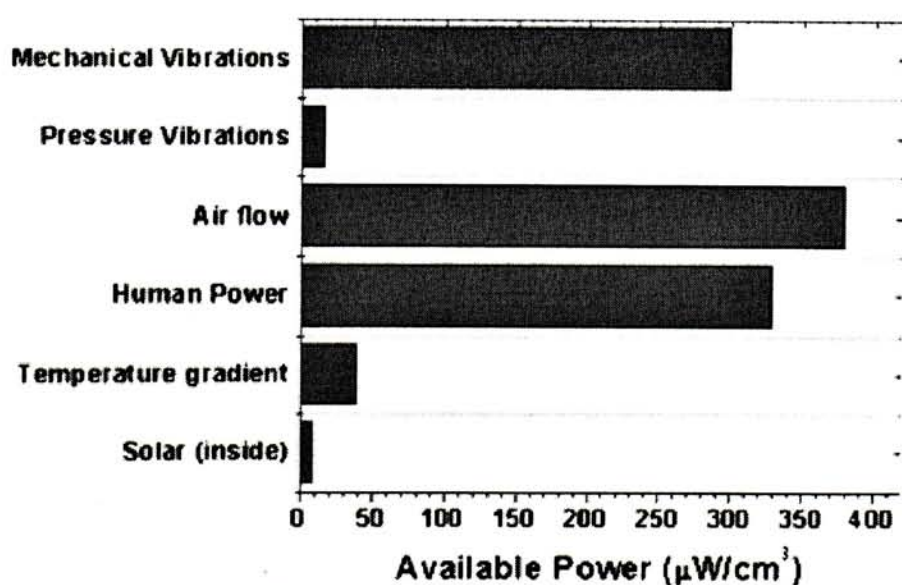


Figure 1.1-1 Comparison of various alternatives for power sources (Priya, 2007)

1.1.3 Piezoelectric energy harvesting

Piezoelectricity produces the charge that accumulates in certain solid materials (notably crystals, certain ceramics, and biological matter such as bone, DNA and various proteins) in response to applied mechanical strain (Skoog et al., 2007). The piezoelectric effect is understood as the electromechanical interaction between the mechanical and electrical states in crystalline materials with no inversion symmetry (Gautschi, 2002).

The piezoelectric effect is a reversible effect. Direct piezoelectricity can generate potential differences of thousands of volts by mechanical effort from external environment applied on the material. One of the best-known applications is the electric cigarette lighter (Vainer, 1976). The key part of electric cigarette lighter is a piezoelectric crystal. The motion of pressing the button will hit the piezoelectric crystal by a spring-loaded hammer. The piezoelectric material can generate a high voltage with electric current that flows across a small spark gap to ignite the gas.

Piezoelectric energy harvesting (PEH) uses piezoelectric materials to convert mechanical energy around the harvester into electrical energy. This energy could then be the energy source for the wireless sensor networks, ICs and even for part of daily electrical power supply in the future. For these reasons, more and more researches devoted to PEH were conducted. Diverse PEH literatures were reviewed or classified by several articles, which cover wide variety of mechanisms and techniques (Sodano et al., 2004; Priya, 2007; Anton and Sodano, 2007).

One of the means of the piezoelectric energy harvesting is human-powered mechanism (Mitcheson et al., 2008; Jia and Liu, 2009). Piezoelectric material can harvest energy from mechanical vibrations by converting mechanical strain into electrical current or voltage. Mechanical vibration exists everywhere in daily life to be exploited for the energy source (Sodano et al., 2004; Beeby et al., 2006; Anton and Sodano, 2007; Rodig et al., 2010), for example, an automobile chassis or jet engine housing. Mechanical excitations widely exist in many situations but can vary widely in frequency and amplitude (Paradiso and Starner, 2005).

The human powered energy harvesting devices use human-based excitations as the energy source for the PEH process, which were characterized as large amplitude and low frequency (Beeby et al., 2006). Mechanical work can be done by translational displacement in the same direction as the force.

Some of the human motions are directly applied by human body, such as footstep or heel strike; while some are closer to harmonic vibration, for example, the limb swing while walking and shaking. Some of the excitations are applied on roadside, highway, railway and pavement. They could also be the energy source by the deformations and vibrations caused by vehicles, trains and pedestrians passing on them.

The East Japan Railway Company (JR-East) has done research on how to make its train stations more eco-friendly. One of the technologies they have worked on is a ticket gate that has piezoelectric elements to generate electricity as commuters walk through. This system relied on a series of piezoelectric elements embedded in the floor under the ticket gates, which generated electricity due to the pressure and

vibration they receive as passengers walk over it. When combined with high-efficiency storage systems, the ticket gate generators could serve as a clean source of supplementary power for the train stations. Busy train stations will be able to accumulate a significant amount of electricity. JR-East claimed that this sort of human-powered electricity generation system may provide a portion of the electricity consumed at train stations in the future.

The heel strike was one of the most investigated motions for human-based PEH because of its large force feature. A well-known piezoelectric shoe insert was developed by MIT's Media Laboratory (Kymissis et al., 1998; Shenck and Paradiso, 2001). They used one PZT dimorph and one PVDF stave to make a shoe insert with complementary conditioning electronics. This device could scavenge energy from compression that was normally goes to waste while walking. The powers harvested at 0.9 Hz walking paces were 8.4 mW and 1.3 mW from the PZT dimorph and PVDF stave, respectively.

The finger strike was also an alternative energy source. Wacharasindhu and Kwon (2008) reported a micromachined energy harvester, which could harvest energy from typing motions on a computer keyboard. It utilized both of piezoelectric and electromagnetic technologies to convert mechanical energy into electrical energy from frequent finger strike motions. The maximum harvested powers were about 40.8 μ W across a 3 M Ω load resistance from piezoelectric conversion and 1.15 μ W across a 35 Ω load resistance from electromagnetic conversion, respectively.

Joint rotation in human body is another potential motion for human-based PEH. Mechanical work at the joint is the product of torque and angular velocity. Therefore, it might be useful if an electric generator can collect some of that work. Knee motion was investigated to be energy harvesting source by Donelan et al. (2008). They proposed a harvester mounted at the knee to generate electricity from the braking phase during walking. Some mechanisms were also utilized to harvest energy from other motions, e.g., the above-mentioned harvesting from keystroke using piezoelectric igniter (Paradiso and Feldmeier, 2001; Tan et al., 2006) and harvesting from limb motion by transforming the swing motion into impacts (Renaud et al., 2009).

Regarding the commercialization of piezoelectric energy harvesting technologies, Innowattech (Abramovich, 2009) has developed a new energy system that harvest mechanical energy imparted to roadways, railways and runways from passing vehicles, trains and pedestrian traffic and convert it into green electricity. Their products called Piezo Electric Generators (IPEG™) were energy scavenging systems which harvest energy that ordinarily goes to waste. According to Innowattech's estimation, IPEG™ has a potential to generate an average power of 200 kWh per hour from the highway with traffic of 600 heavy trucks/buses per hour on average.

The above mentioned human motion driven energy harvesters are generally based on the force in the vertical direction. Some energy associated with the torsion motion can also be harvested. Priya et al. (2005) reported “Piezoelectric Windmill” for generating the electrical power from wind, which was utilized for rotary working condition. Figure 1.1-2 shows the piezoelectric windmill. Priya (2005) has proposed a model for

this piezoelectric windmill. The piezoelectric energy transducers were arranged in disk type structure. At the wind speed of 10 mph, a power of 7.5 mW was recorded across a matching load of 6.7 k Ω .

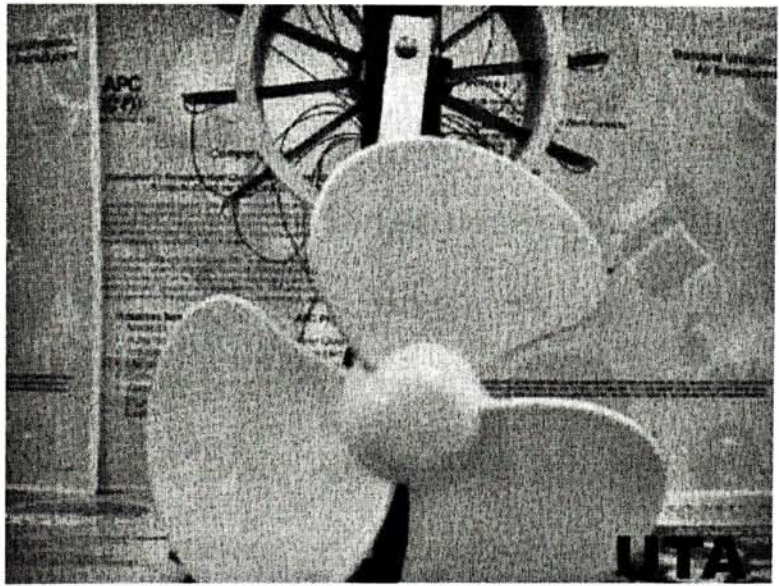
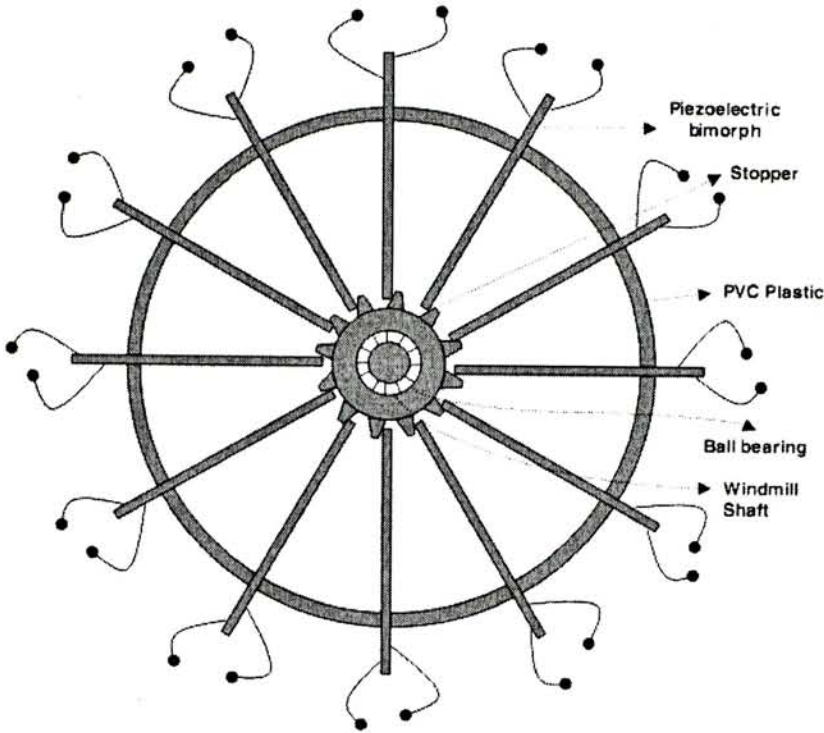


Figure 1.1-2 Schematic and picture of fabricated prototype “Piezoelectric Windmill” (Priya et al., 2005)

1.1.4 Impact based piezoelectric energy harvester

In most machines and dynamic systems, kinetic energy exists in the form of vibrations, regular or random displacements, and driving forces (Khaligh et al., 2010). The excitations for vibration based piezoelectric energy harvesting devices were discussed. The sources of excitations for vibrations are diverse. Most of the analyses on PEH reported in the literature were limited to a steady-state approach to the problem. These analyses may not give clear insights when the dynamical behaviors of the piezoelectric bender are governed by its transient characteristics, for example in the case of a shock or impact excitation (Renaud et al., 2007).

The impulse given by the falling down steel ball or moving object was investigated by researchers. Earlier investigation to harvest energy from mechanical impacts using piezoelectric materials was introduced by Umeda et al. (1996, 1997, and 2003). They proposed a systematic analysis of the energy generated by the impact of a 5.5 g steel ball at the height of 20 mm onto a piezoelectric structure. The piezoelectric structure was composed of a bronze plate in 27 mm diameter and piezo-ceramics in 19 mm diameter, with 0.25 mm thickness. The harvested energy was estimated by a resistive load that was directly connected to the piezoelectric element. Later work involved the standard AC-DC convertor for energy harvesting. Umeda et al. (1997) concluded that the harvested efficiency was greatly related to the initial rectified voltage. These works done by Umeda et al. were typical investigation and contribution to the impact based vibration energy harvesting. They introduced an electrical equivalent model to simulate the energy generation mechanism. Vibration models were also provided. One was a model with the transducer and the steel ball, the other was only focused on the

transducer part. The steel ball provided an impact excitation to the energy harvesting system so that it caused the cantilever to vibrate. This type of impact excitation energy harvester has been used in devices such as a piezoelectric transducer designed by Renaud et al. (2009).

Renaud et al. (2009) have designed an improved energy harvester, as shown in Figure 1.1-3. In this paper, they have reported a device for transforming part of the mechanical energy from human limb motion into electrical energy. It consisted of a basic frame with a channel that allowed a free sliding mass to move along it. There were also two piezoelectric cantilevers positioned at the ends of the frame. When the frame was shaken along the direction of the channel, the sliding mass would hit the piezoelectric cantilevers occasionally. Then part of the kinetic energy transferred by the mass was converted into electrical energy by the piezoelectric cantilevers through the impact process. An analysis of the system dynamics was coupled to a model of the piezoelectric transducer to evaluate device performances. An optimized power output was around several hundred micro Joules and 10% conversion efficiency.

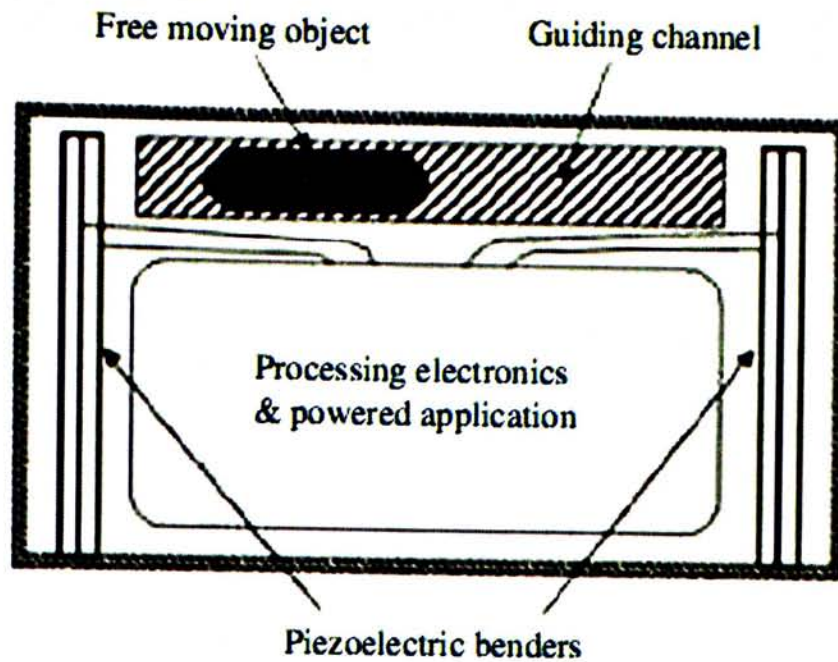


Figure 1.1-3 Conceptual representation of the impact-based vibration energy harvester (Renaud et al., 2009).

Most of these existing researches took the falling down steel ball as the impact excitation in the system. Another excitation such as an impact-driven, coupled vibration energy harvester was also investigated (Gu and Livermore, 2011).

The above mentioned researches were focused on energy generation capabilities. Ng and Liao (2005) demonstrated that the instantaneous power harvested by the piezoelectric vibrating structure was too small to be used in practical applications. Therefore, the energy harvesting circuit and storage devices were necessary for PEH. Some of the extracted energy was dissipated during the process, while the rest of extracted energy would be harvested and stored in some suitable electrical energy storage devices (Sodano et al., 2005a, b; Guan and Liao, 2007, 2008).

The harvesting circuit plays an important role in PEH and the efficiency optimization. In the previous studies, Umeda et al. (1997) introduced rectifiers to extract energy from vibrating piezoelectric structures. Ottman et al. (2002, 2003) proposed a two-stage harvesting circuit by implemented a DC-DC converter for adapting the rectified voltage to maximum harvesting power. Guan and Liao (2007) pointed out that the one-stage harvesting circuit could have higher efficiency than the two-stage harvesting circuit. The energy harvesting efficiency was found to be 46% with the power harvesting circuit operating in so called “burst mode”.

The impedance matching theory is useful in load power optimization. Liang and Liao (2010) extended the impedance matching theory to provide the methodology for obtaining the equivalent impedances of the PEH device. By the energy flow chart, Liang and Liao (2009) have clarified the definitions of energy harvesting and energy dissipation in PEH. They compared standard energy harvesting with resistive shunt damping to illustrate the concepts. Furthermore, they have also pointed out that both of the harvested and dissipated energy changed with the rectified voltage, the energy flow chart (Liang and Liao, 2011) was also useful when considering mechanical to electrical energy harvesting process.

Wu et al. (2009) have compared three energy harvesting circuits with resistive load case. And their results showed that synchronized switching and discharging to a storage capacitor through an inductor (SSDCI) produced 200% the output power of the resistive load case.

1.1.5 Operation of piezoelectric materials

Basically, there are two operation modes for piezoelectric materials in applications. Before defining these two modes, we should state one important property of piezoelectric materials. An electric field can be applied after the material was poled to induce an expansion or contraction of the material. However, the electric field can be applied in any direction, each resulting in a potentially different stress and strain generation (Sodano et al., 2004). Hence, it is necessary to specify the piezoelectric properties in three directions when applying electric potential.

The typical piezoelectric structures used to convert mechanical vibration into electrical energy include one or several piezoelectric layers, which form as sandwich structure between metallic electrodes and acting as capacitors. These piezoelectric capacitors can be arranged in parallel or in series. They can be connected to the electric power storage devices through rectifiers.

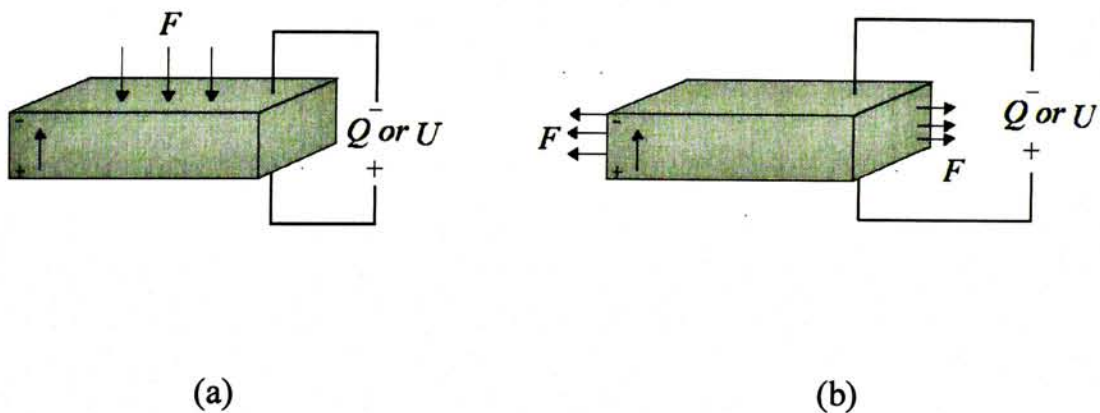


Figure 1.1-4 Schematic illustration of the piezoelectric direction of forces applied and voltage generated in two operation modes (a) d33 mode; (b) d31 mode

With the assumption that the poling direction is in direction '3' (axis '3'), the piezoelectric energy harvesting can be generally divided into two modes. The first one is the bender that operates in '31' mode and the other is the stack configuration that is so called '33' mode. In the 31 mode, the principal deformation is in the '1' direction and the electric field is applied in the '3' direction. In the 33 mode, the strain is mainly occurring in the '3' direction, which is the same as the poling direction. Figure 1.1-4 shows the schematic illustration of the piezoelectric direction of forces applied and voltage generated in two operation modes.

With this definition on the operation modes of piezoelectric materials, the electromechanical coupling coefficients d and g can be defined. In the actuation case, the major coefficient considered is d , and in the sensor, g is of major concern.

1.2 Research Objective

Rotary motions widely exist in the world, for examples, windmill, rotary entrance gates, turnstiles in ticket gates in railway and subway stations and entrance turnstile gates in supermarkets or parks. Wind flow is a large potential energy source. The passenger flow in railway and subway stations, parks and supermarkets is another potential energy source to be exploited, in particular, for a metropolitan city with huge population such as Hong Kong. One of the most convenient transportation means for commuters is railway and metro in daily life. According to the statistics by MTR of Hong Kong, the monthly patronage can achieve about one hundred million in 2011. Such high patronage makes the turnstiles to be a very promising energy source.

In this thesis, a new energy harvesting device will be designed to scavenge energy from rotary devices, which can be utilized in windmills, rotary entrance gates, and ticket gates in metro stations and supermarkets. Figure 1.2-1 shows two kinds of energy sources associated with rotary motions.

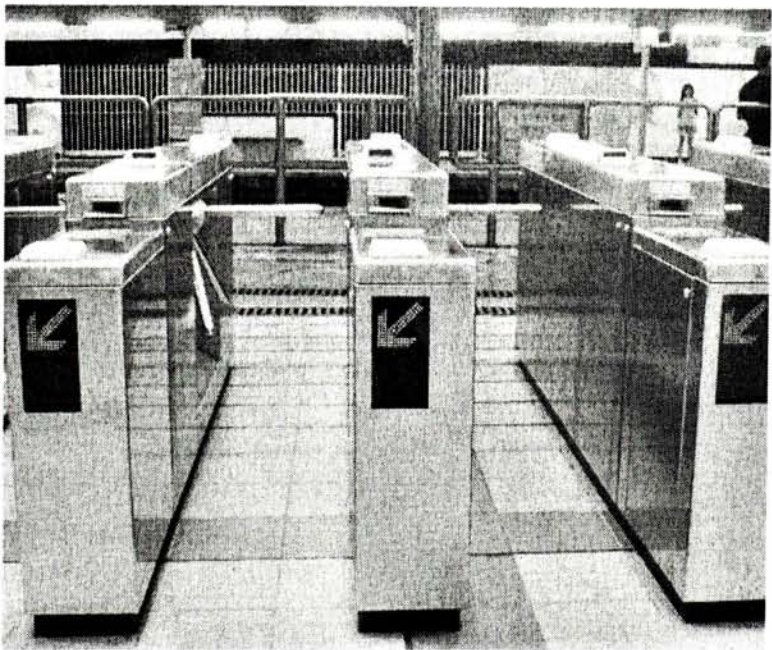
Generally speaking, there are two types of gates utilized in railway stations and supermarkets in Hong Kong. One is automatic ticket gate, which consumes electric power to drive it open or shut. The other is the turnstile type. It is driven by passengers or customers when they pass the gate. Turnstile can just let one passenger or customer pass it for one time. So in the railway or subway stations it can effectively avoid passengers from stealing a ride, which may be a problem for an automatic gate because it may let more than one passenger pass the gate for one ticket. Therefore, there is only one or two automatic gates in each exit for passengers who

carry extra big luggage. Hence, turnstiles are popular in Hong Kong railway and subway stations, parks and supermarkets.



(a) Windmills

(http://www.copper.org/applications/electrical/energy/casestudy/wind_energy_a6101.html)



(b) Turnstile ticket gates in Hong Kong railway stations

Figure 1.2-1 Potential energy sources for rotary energy harvesting.

The existing rotary energy harvester such as piezoelectric windmill structure could be used for energy harvesting from rotary motions. However, since all piezoelectric cantilevers are hit at the same time so that the resistance of the whole structure could be high. Therefore, the required force to drive the structure to rotate would be relatively high. Suppose there are n piezoelectric cantilevers and n plectra in the windmill, then if the windmill turns for one round, every piezoelectric cantilever will be hit n times. The impact frequency is the reciprocal of the time interval between every two impacts. Therefore, the rotational on each piezoelectric cantilever is n times of the rotational frequency of the rotary energy harvester (REH). When the rotational frequency of the REH is high, the impact frequency will be even much higher than rotational frequency of the REH.

This thesis proposes an extended rotary energy harvester (E-REH) using multiple piezoelectric cantilevers. It is made of several pieces of piezoelectric bimorph cantilevers that are arranged in parallel, and a rotary cylinder with plectra distributed on it. The cylinder is connected with the rotary shaft of the input energy source. The rotary motion of the energy source drives the cylinder to rotate so that the plectra on it will hit their corresponding bimorphs to vibrate. This vibration of piezoelectric bimorph cantilevers will continuously generate electricity.

1.3 Thesis Organization

This thesis consists of five chapters. It is organized as follows:

In Chapter One, background of energy harvesting is introduced. Literature on energy harvesting technology is reviewed. Research objective is stated;

In Chapter Two, design considerations of an extended rotary energy harvester (E-REH) are provided. An analytical model based on impact force is developed. Simulation results are also given. The model can serve for prediction and analysis on the output power performance of the energy harvester;

In Chapter Three, a prototype is fabricated and experiments are set up. The output voltage and power across resistive load under different experiments are carried out and the results are recorded. The corresponding simulation results are compared with the experimental data;

In Chapter Four, the power output performance is analyzed and compared between E-REH and REH structures under different input conditions. Possible applications for both designs are discussed;

In Chapter Five, conclusion and future work are summarized.

CHAPTER TWO DESIGN AND MODELING OF AN EXTENDED ROTARY ENERGY HARVESTER

This chapter presents the design and modeling of an extended rotary energy harvester (E-REH). Design concept of the rotary cylinder with plectra is introduced. Impact based vibration model for the device is developed. Simulation results on output voltage and power with varying tip displacement and impact frequency are obtained.

2.1 Design Considerations of an Extended Rotary Energy Harvester

Rotary energy harvesting apparatus are not as diversiform as the vertical energy harvesting devices. Nevertheless, rotary motions exist widely in daily life as well. The rotary motions could also be the energy sources for energy harvesting by transferring mechanical motions into electrical energy via piezoelectric cantilevers.

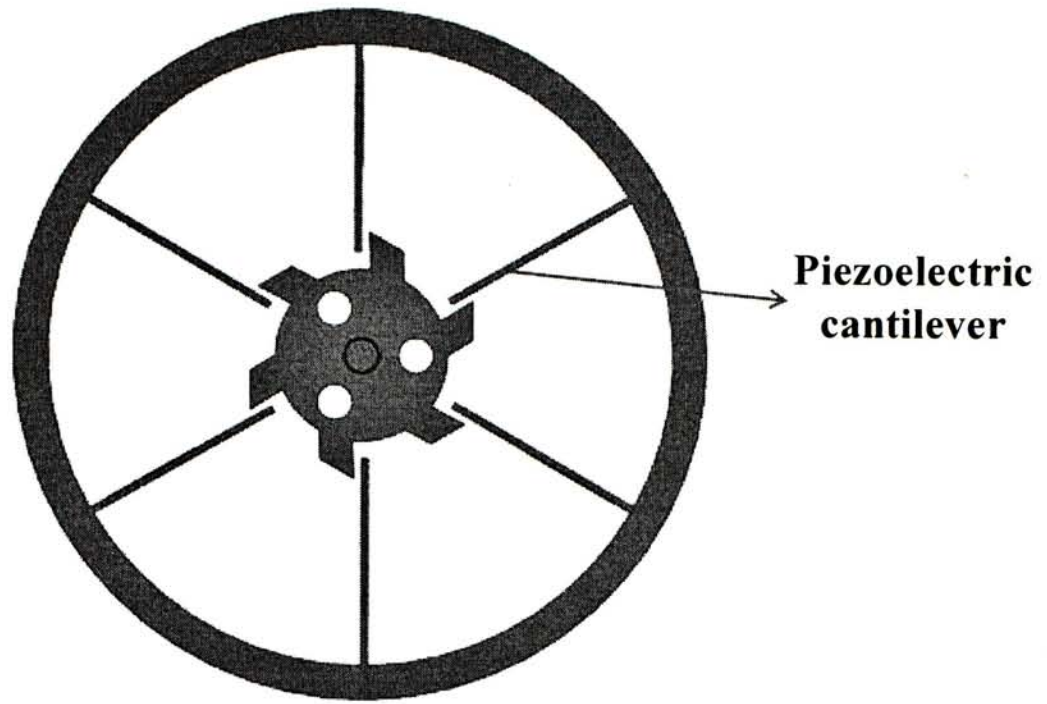


Figure 2.1-1 Schematic design of the rotary energy harvester (REH)

One of the available designs for rotary energy harvesters (REH) using piezoelectric cantilevers is to arrange the cantilevers along the circumference of a disk. The schematic design of REH is shown in Figure 2.1-1. The piezoelectric windmill by Priya et al. ([2005](#)) is this kind of structure for harvesting energy from wind. The alternating mechanical stress is trapped and applied on the piezoelectric cantilevers, which can convert the mechanical energy into electrical energy by direct piezoelectric effect. Then the electricity is stored or consumed by the load. This structure used several piezoelectric bimorph cantilevers. It can bear large input force because all of the piezoelectric bimorph cantilevers share the force at the same time. Each piezoelectric bimorph cantilever has one corresponding plectrum. Therefore, if there are n pieces of piezoelectric bimorph cantilevers working in the structure, then each piezoelectric bimorph is impacted for n times for one round rotation. This introduces

an amplification effect on the rotational frequency for a rotation source with a certain rotational frequency. However, the amplification effect on rotational frequency could be a problem under high rotational frequency input source.

A design called extended rotary energy harvester (E-REH) is proposed to possibly avoid the disadvantage of the above rotary energy harvester (REH). Figure 2.1-2 shows the schematic design of the rotary part with distributed plectra, which are connected with the shaft.

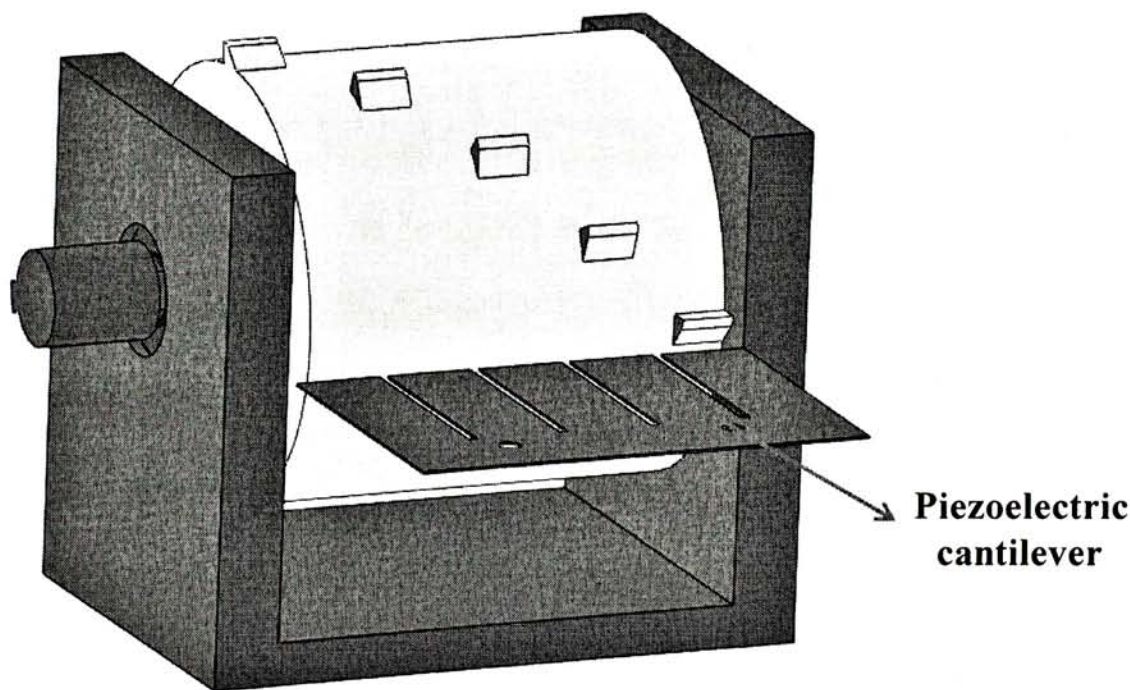


Figure 2.1-2 Schematic design of the extended rotary energy harvester (E-REH)

In REH, piezoelectric bimorph cantilevers are arranged around the circumference of the central shaft. Firstly, the required force to drive the structure is the total restoring force from n piezoelectric cantilevers. Secondly, when the rotary shaft in REH rotates for one cycle, each one of piezoelectric cantilevers will be impacted for n times by all of the plectra on the rotary shaft. The impact frequency on piezoelectric bimorph cantilevers in REH structure is n times of the rotational frequency of the rotary shaft in REH.

In E-REH, an extended distribution of plectra on a rotary cylinder is designed as shown in Figure 2.1-2. For the configuration, n pieces of piezoelectric bimorph cantilevers are arranged in parallel. Plectra are arranged in E-REH so that the impact frequency on piezoelectric cantilevers is equal to the rotational frequency. Furthermore, input force can be applied on the piezoelectric bimorph cantilevers one by one. Mechanical deformation will be caused by the force. Tip displacement of the cantilever would be close to the maximum allowable deformation in order to obtain maximum power output.

2.2 *Models of Rotary Energy Harvesters*

Multiple piezoelectric bimorph cantilevers are both utilized in E-REH and REH. Analysis for the piezoelectric unimorphs and bimorphs were investigated by several researchers (Smits and Choi, 1991; Wang and Cross, 1999; Huang et al., 2004; Renaud, 2007; Ajitsaria, 2007). An analytical model will be developed to predict the performances of such an impact based piezoelectric energy harvester. Impact force is applied by the plectrum corresponding to each piezoelectric bimorph.

In order to investigate the impact-based vibration energy harvesting systems, it is important to indentify the basic types of impact or collisions, which require distinct methods of analysis. Different collision causes different distribution of deformation even influences the period of contact in each of the colliding bodies. There are four types of analyses in general, associated with particle impact, rigid body impact, transverse impact on flexible bodies (i.e. transverse wave propagation of vibrations), and axial impact on flexible bodies (Stronge, 2000).

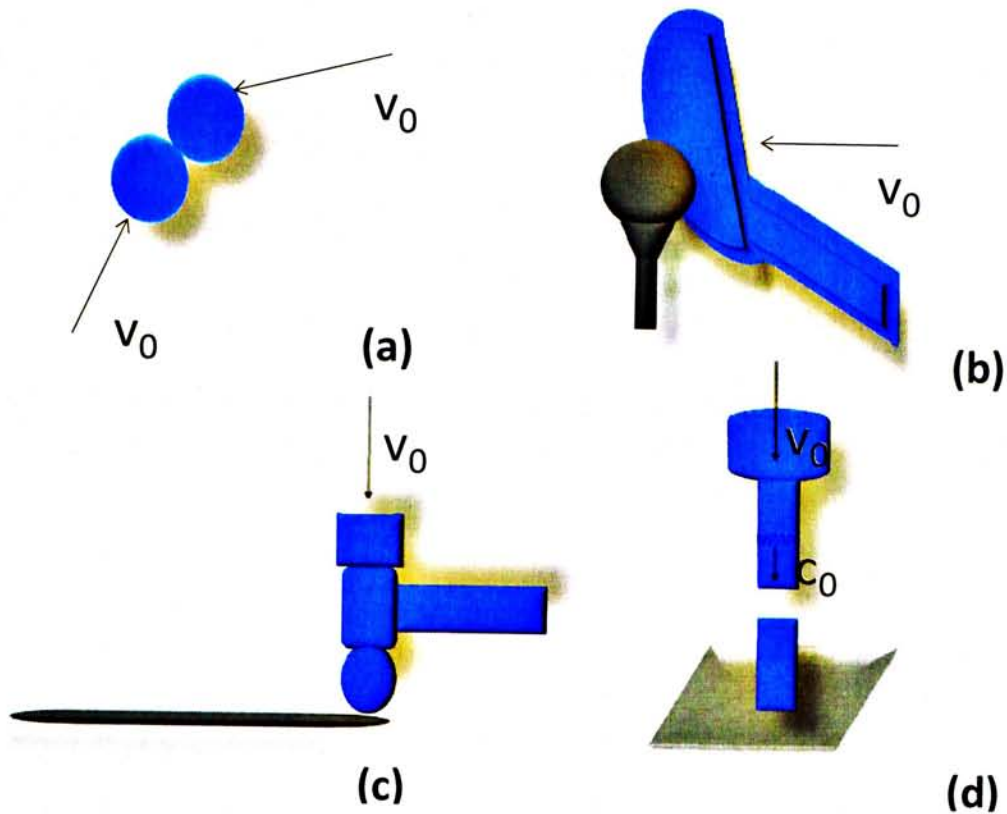


Figure 2.2-1 Four general impact problems: (a) particle impact (stereo-mechanical), (b) rigid body impact, (c) transverse deformations of flexible bodies, and (d) axial deformation of flexible bodies ([Stronge, 2000](#)).

- (a) **Particle impact** is an analytical approximation that considers a normal component of interaction impulse only. Both particles are smooth and spherical. The source of the interaction force is unspecified and has very short range so that the period of interaction is negligibly small.
- (b) **Rigid body impact** happens between compact bodies when the contact area and deformation both remain small. The stresses generated in the contact region decrease rapidly with increasing radial distance from the contact area. The deformation is small but large stiffness will separate the two contacted bodies.
- (c) **Transverse impact on flexible bodies** occurs when at least one of the bodies suffers bending as a result of the pressures happened in the contact area. This

bending reduces the interface pressure and prolongs the period of contact. This category is the most relevant in the analysis of our energy harvester.

(d) **Axial impact on flexible bodies** is not of interest in our research.

The analysis of our structure is generally based on (c) as stated above. A pulse force is applied on the piezoelectric bimorph cantilever with velocity v_0 and relatively impact frequency f .

This model could describe the impact-based vibration of a piezoelectric bimorph cantilever. The performances of the energy harvester can then be estimated. The advantages and scope of applications of the energy harvester can also be discussed by using this model for the output power performances.

The model will be developed based on the following assumptions:

1. Linearity of the constitutive equations relating mechanical and electrical variables;
2. Displacement at the free end of the bimorph (tip displacement) is small;
3. Interface between the plectrum and piezoelectric layer is frictionless;
4. The mechanical input applied to the harvester can be represented by a concentrated force.

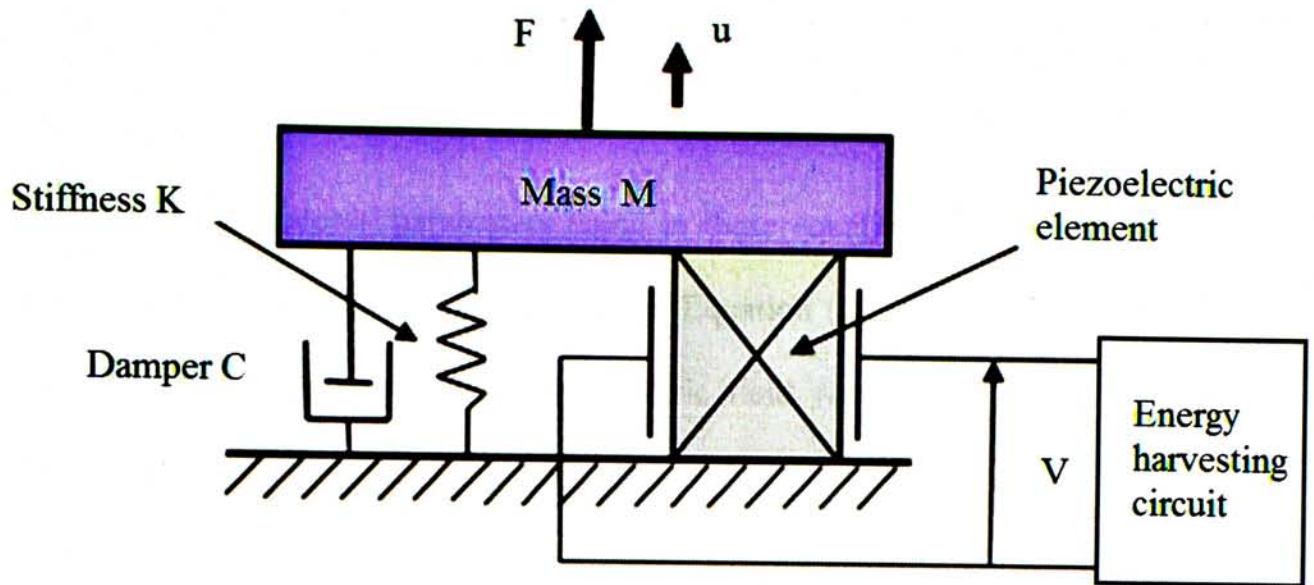


Figure 2.2-2 Equivalent model of a vibrating structure with bonded piezoelectric elements ([Badel et al., 2005](#))

A vibrating piezoelectric bimorph cantilever can be approximated to be a piezo-mass-spring-damper system as shown in Figure 2.2-2. The area of the location that is applied impact force is small with respect to that of the whole surface. So the impact force is concentrated on the collision surface. This impact force is assumed not to be affected by the vibrating cantilever during the contact process. So it can be described as a pulse function.

To analyze the dynamics of piezoelectric devices, a common description on the piezoelectric materials is considered. As given in the IEEE Standard on Piezoelectricity ([1988](#)), the linear piezoelectricity can be represented by the constitutive equations as follows:

$$\begin{bmatrix} T_p \\ D_i \end{bmatrix} = \begin{bmatrix} c_{pq}^E & -e_{kp} \\ e_{iq} & \epsilon_{ik}^S \end{bmatrix} \begin{bmatrix} S_q \\ E_k \end{bmatrix} \quad (2.2-1)$$

The piezoelectric material parameters using in these equations are defined in Table 2.2-1. Equation (2.2-2) can be obtained from Equation (2.2-1) where T is the stress vector, S is the strain vector, E is the electric field vector, and D is the electric displacement vector (Badel et al., 2005).

$$\begin{cases} T = c_{33}^E S - e_{33} E \\ D = e_{33} S + \epsilon_{33}^S E \end{cases} \quad (2.2-2)$$

Table 2.2-1 Definitions of piezoelectric material properties

c_{33}^E	Elastic rigidity of the piezoelectric element short-circuit
c_{33}^D	Elastic rigidity of the piezoelectric element open-circuit
ϵ_{33}^S	Clamped permittivity of the piezoelectric element
ϵ_{33}^T	Free stress permittivity of the piezoelectric element
e_{33}	Piezoelectric coefficient of the piezoelectric element
A	Cross sectional area of piezoelectric element
L	Thickness of piezoelectric element

The relationship between the mechanical and electrical fields Equation (2.2-3) can be consequently derived from Equation (2.2-2):

$$\begin{aligned} F_p &= K_{PE} + \alpha V \\ I &= \alpha \dot{u} - C_0 \dot{V} \end{aligned} \quad (2.2-3)$$

$$E = -\frac{V}{L}, \quad S = \frac{u}{L}, \quad I = A\dot{D}, \quad F_p = AT \quad (2.2-4)$$

Equation (2.2-3) links the mechanical variables and the electrical ones. F_p is the internal force due to the piezoelectric element. I and V are the output current and voltage on the piezoelectric element connected to the energy harvesting circuit. K_{PE} is the short-circuited stiffness of the piezoelectric element, α is the force factor, and C_0 is the clamped capacitance of the piezoelectric element.

As the restoring forces due to both of the stiffness of the mechanical structure and the stiffness of the piezoelectric element act in the same way on the mass M , a total short-circuited stiffness can be defined as

$$K_E = K_{PE} + K_S \quad (2.2-5)$$

Equation (2.2-6) defines the dynamics of the system as follows:

$$M\ddot{u} = F - K_E u - \alpha V - C\dot{u} \quad (2.2-6)$$

$$\alpha = \gamma C_0, K_E = \alpha \gamma \frac{f_0^2}{f_1^2 - f_0^2}, M = \frac{K_E}{4\pi^2 f_0^2}, C = 4\pi^2 M f_1^2 \quad (2.2-7)$$

The displacement at the free end of piezoelectric cantilever is u , C is structural damping coefficient, F is the external force applied to the structure, and M is the effective mass because no extra mass is attached on the cantilever in our case.

The clamped capacitance of the piezoelectric material is measured by the Impedance Analyzer (HP 4294) while using the equivalent circuit (Liang and Liao, 2010) shown in Figure 2.2-3. Measurement results are shown in Figure 2.2-4.

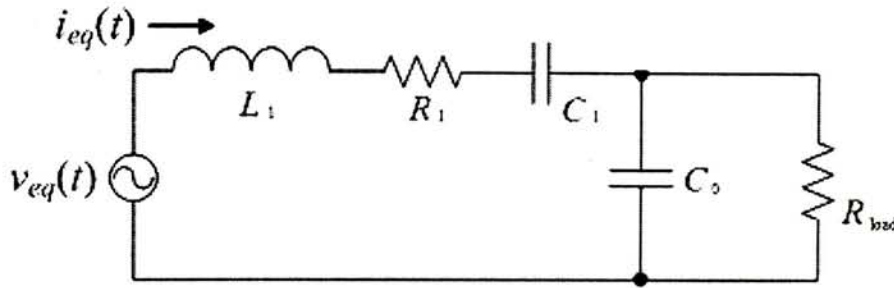


Figure 2.2-3 Equivalent circuit of PEH device

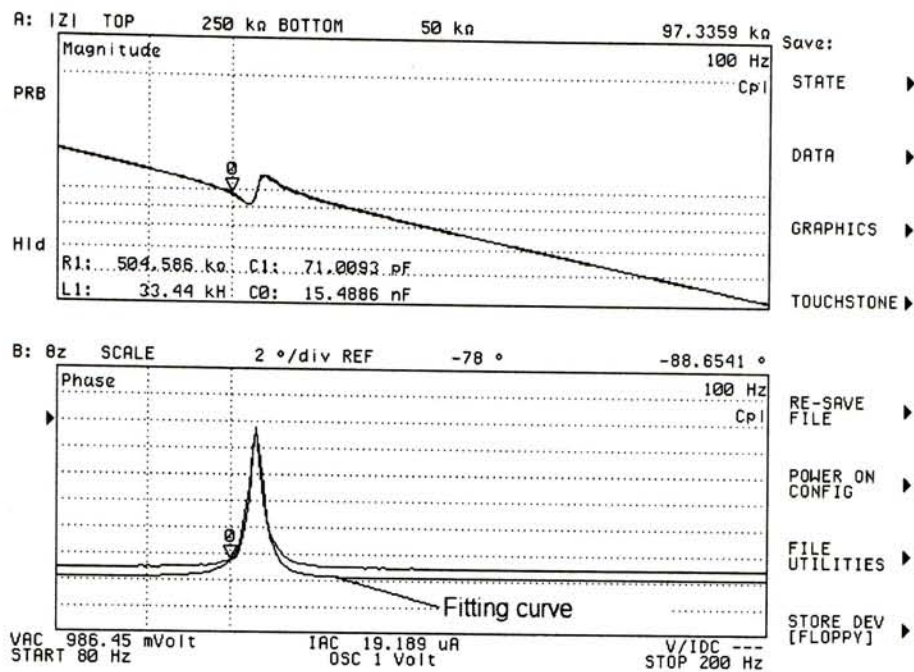


Figure 2.2-4 Impedance properties measured by impedance analyzer

Considering the piezoelectric vibrating structure, the values of various parameters considered in this model can be obtained from experiments. Parameters can be expressed by Equations (2.2-8) using experimental measurements defined in Table 2.2-2.

Table 2.2-2 Definitions of parameters and constants

f_0	Short circuit resonance frequency
f_1	Open circuit resonance frequency
ξ	Open circuit damping coefficient
C_0	Clamped capacitance of the piezoelectric bimorph
γ	Piezoelectric open circuit voltage to the beam free end displacement ratio

When considering the open circuit output voltage or the voltage across the resistive load, Equation (2.2-3) becomes Equations (2.2-8) and (2.2-9), respectively.

$$\alpha \dot{u} - C_0 \dot{V} = 0 \quad (2.2-8)$$

$$\alpha \dot{u} - C_0 \dot{V} = \frac{V}{R_L} \quad (2.2-9)$$

Therefore, a mechanical structure with bonded piezoelectric elements is modeled by solving Equations (2.2-6) and (2.2-8) or (2.2-9). The input force is simplified as a pulse function. The pulse period is $T = \frac{1}{f}$, where f is the pulse frequency. The width of the pulse is decided by the time during the contact between the plectrum and the tip of the piezoelectric cantilever. Figure 2.2-5 shows the corresponding Simulink model.

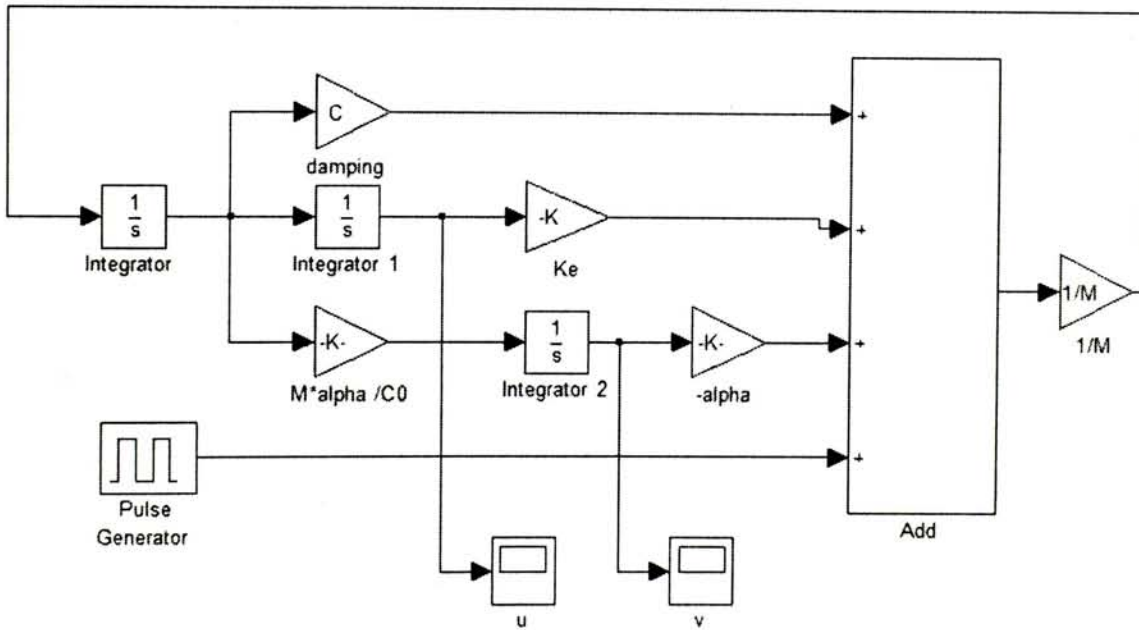


Figure 2.2-5 Simulink model for impact based rotary energy harvester

2.3 *Simulation Results*

Parameters defined in Table 2.2-2 are measured by experiments and given in Table 2.3-1. The outer dimensions of the piezoelectric bimorph cantilever are $41.40 \times 17.02 \times 0.76 \text{ mm}^3$. Simulation results are obtained using those parameters. Figure 2.3-1 shows the simulation result when the rotational frequency is 1 Hz; the maximum tip displacement is 0.7 mm by setting the overlap distance between the edge of the plectrum and the tip of the cantilever. Figure 2.3-2 shows the simulation result when the rotational frequency is 2 Hz and the maximum tip displacement is 1.4 mm.

Table 2.3-1 Parameter values

f_0	100.5 Hz
f_1	102.5 Hz
ξ	0.0024
γ	150,000 V/m
C_0	15.5 nF

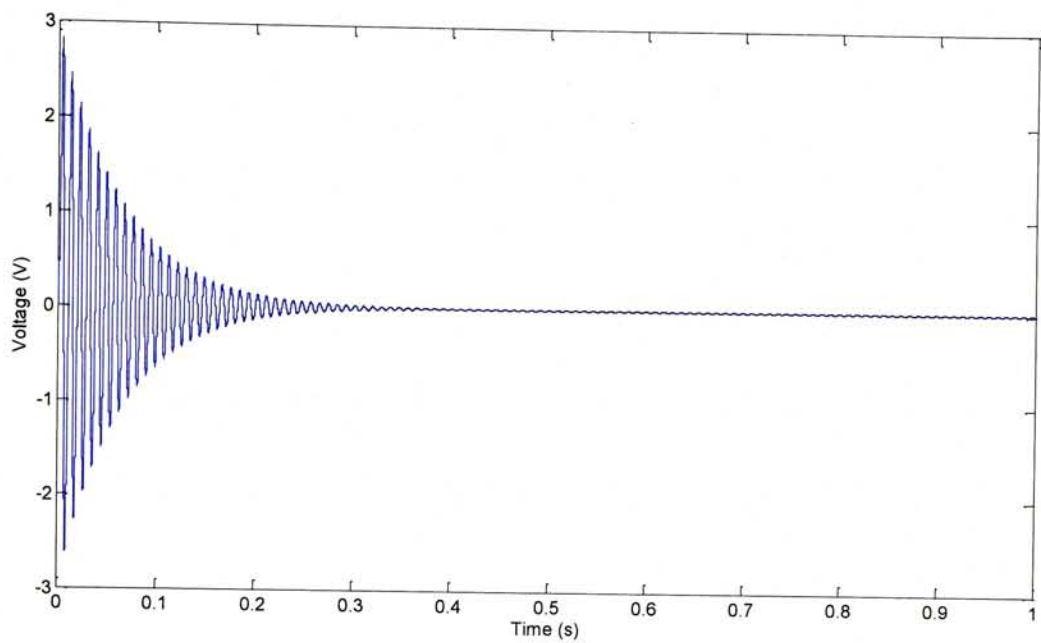


Figure 2.3-1 Time response of the output voltage (1 Hz rotational frequency, $u_{max} = 0.7$ mm)

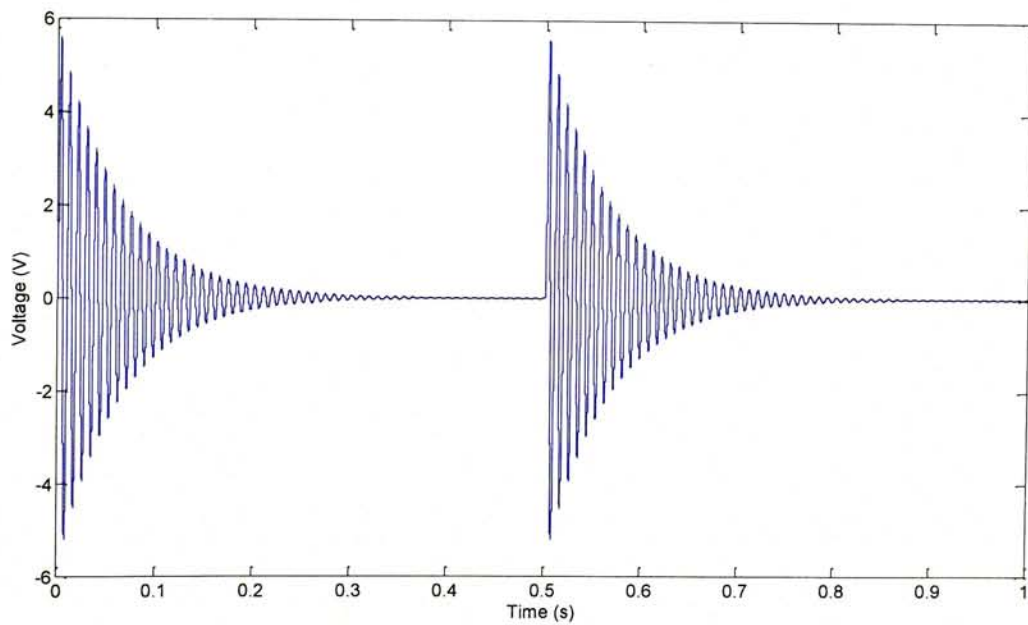


Figure 2.3-2 Time response of the output voltage (2 Hz rotational frequency, $u_{max} = 1.4$ mm)

The average output power across the resistive load is calculated by

$$P = \frac{1}{T} \cdot \int_0^T \frac{V^2}{R} dt \quad (2.3-1)$$

where T is the time interval between every two impact, R is the resistive load. Output power with varying tip displacement under 0.78 Hz rotational frequency is obtained and shown in Figure 2.3-3. It can be seen from the figure that the output power increases with the maximum tip displacement. The output power with varying rotational frequency is also obtained and shown in Figure 2.3-4. It can be seen that the output power also increases with increasing rotational frequency.

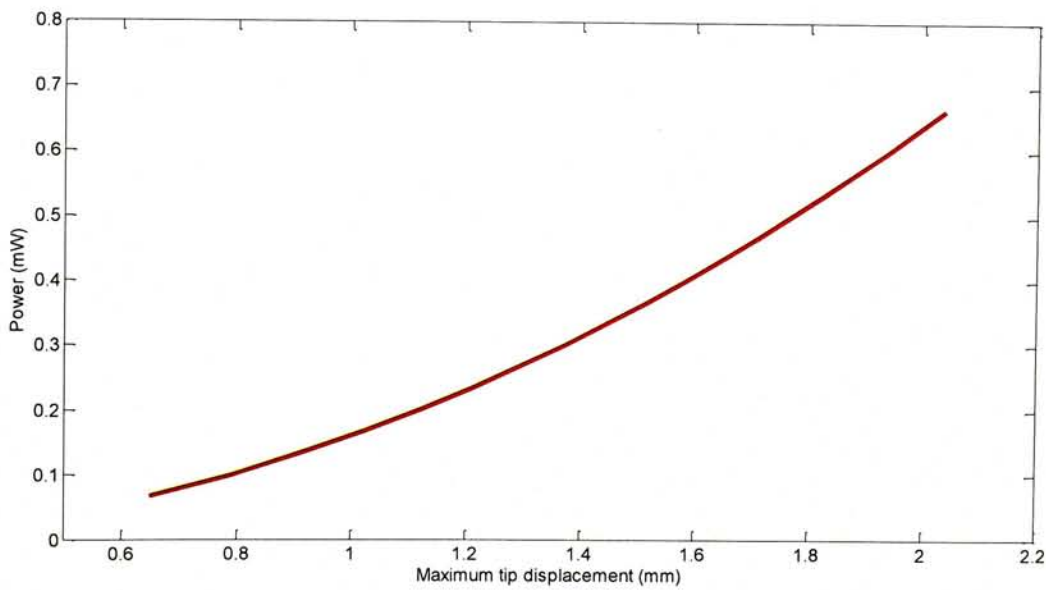


Figure 2.3-3 Output power versus maximum tip displacement ($f = 0.78$ Hz)

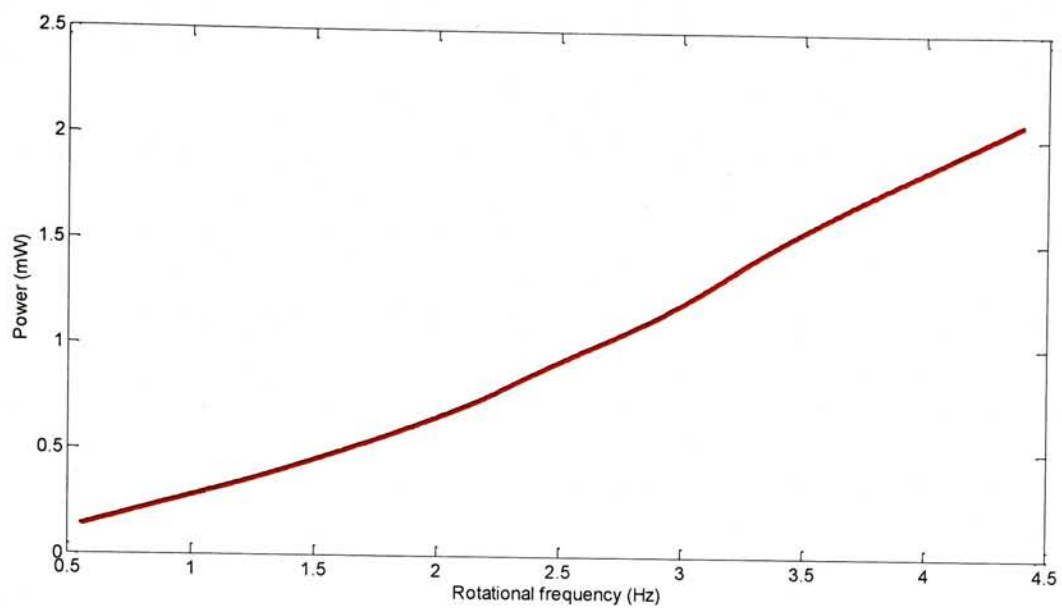


Figure 2.3-4 Output power versus rotational frequency ($u_{max} = 1.5$ mm)

2.4 *Chapter Summary*

An extended rotary energy harvester (E-REH) was proposed and designed. An analytical model for the rotary energy harvester was developed. The model was based on the linear piezoelectricity and the equivalent circuit of the piezoelectric material. Simulation results of output voltage were obtained. Output power versus tip displacement and rotational frequency were also simulated by the model.

CHAPTER THREE PROTOTYPE, TESTING AND OUTPUT POWER OF EXTENDED ROTARY ENERGY HARVESTER

In this chapter, a prototype of the extended rotary energy harvester (E-REH) will be fabricated and tested. Experimental setup will be provided. The output voltage of the E-REH will be evaluated. The developed model will be validated by experimental data. The output power performances with varying maximum tip displacement of the piezoelectric bimorph cantilever and varying rotational frequency will be investigated.

3.1 *Prototype and Experiment*

Figure 3.1-1 shows the prototype of the rotary cylinder with plectra. The plectra are distributed on the surface of the cylinder. The radius and length of the cylinder are 50 mm and 100 mm, respectively. The width and height of each plectrum are 12 mm and 5 mm, respectively. The axial space between every two adjacent plectra is 22 mm. This prototype is made by rapid prototyping. Piezoelectric bimorph cantilevers are arranged in parallel as shown in Figure 3.1-2.

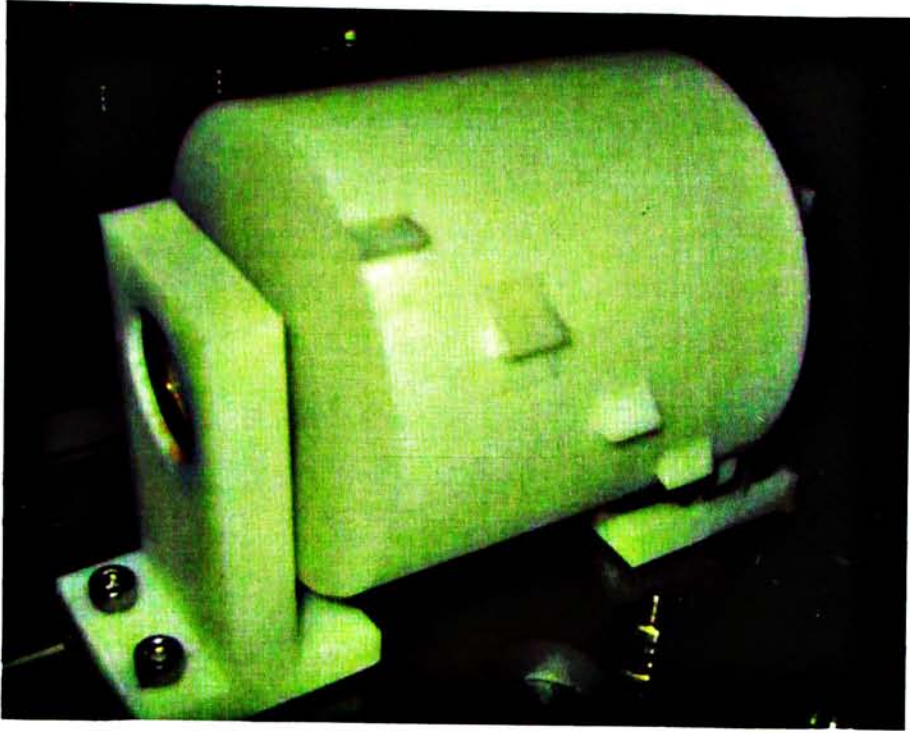


Figure 3.1- 1 Prototype of E-REH

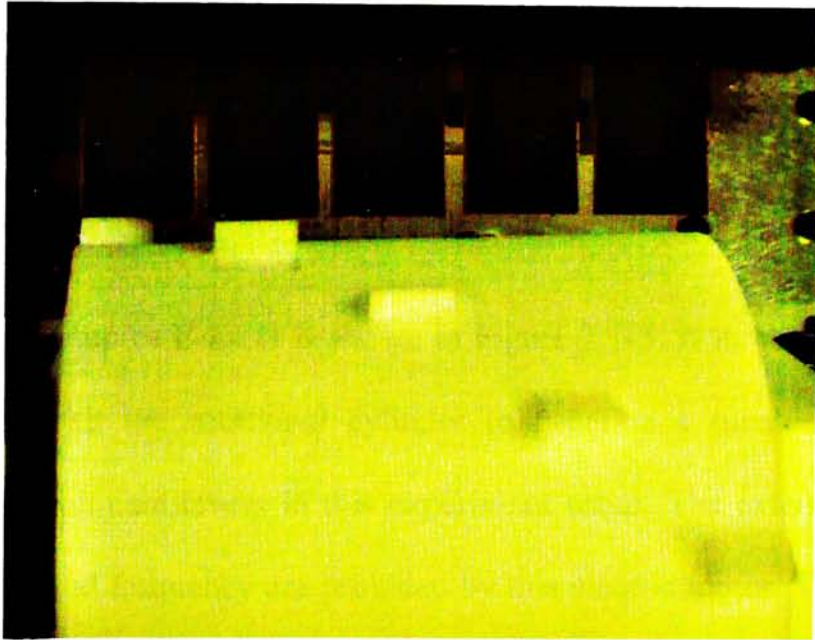


Figure 3.1-2 Piezoelectric bimorph cantilevers arranged in parallel

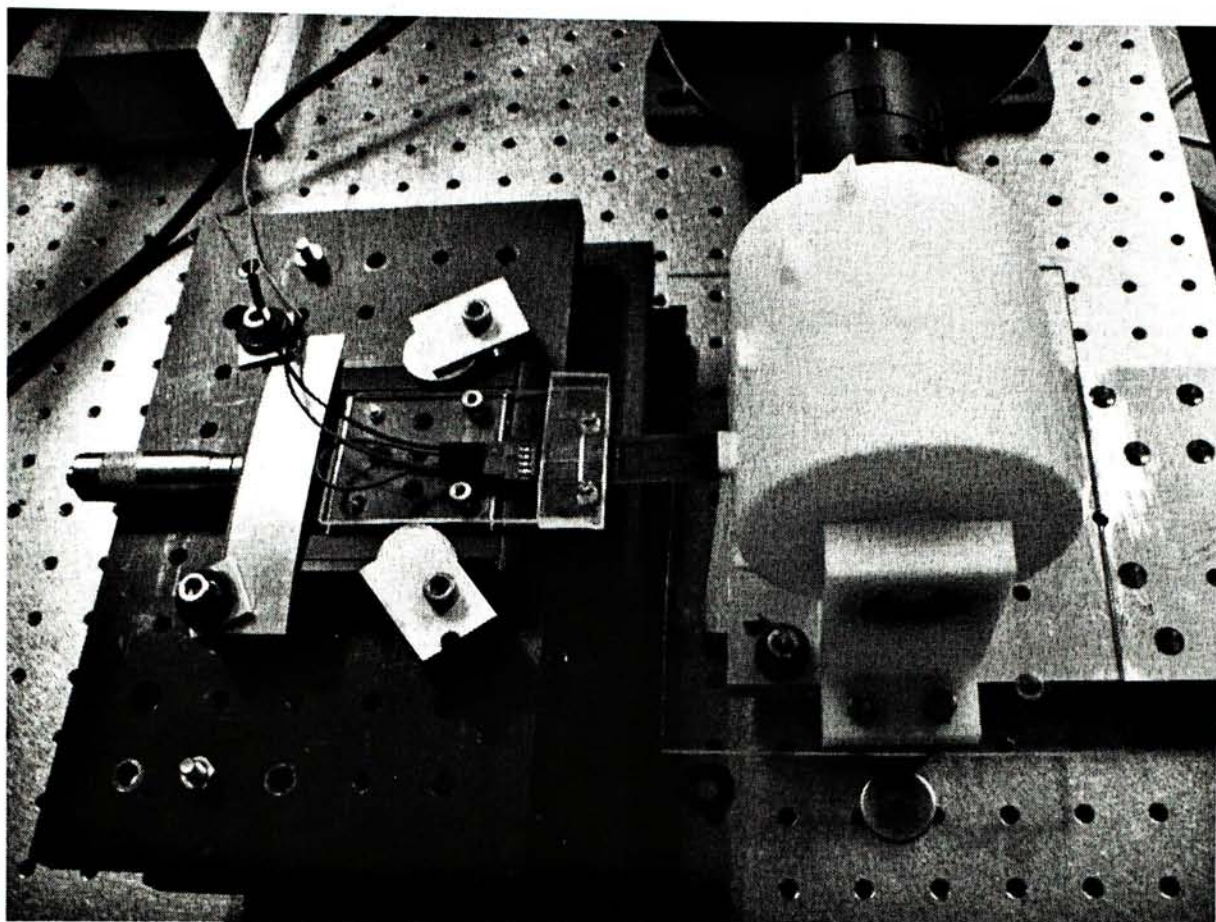


Figure 3.1-3 Experimental setup of E-REH

The experimental setup of E-REH is shown in Figure 3.1-3. A motor (AEG AM 100 L) is connected with the rotational cylinder to generate a tunable force on the piezoelectric bimorph cantilevers in this experiment setup. The external forces with various amplitude and frequency are provided by this electric motor. The motor has a controller that can tune the output of the motor. The display value on the motor controller and the actual rotational frequency has a relationship $f = 0.474\nu + 0.307$, where ν is the value on the display panel of motor controller. Components in the experimental setup include:

- 1) DC motor
- 2) Rotational cylinder with distributed plectra
- 3) Piezoelectric bimorph cantilevers
- 4) Holder for the bimorph cantilevers with micrometer stand

The whole setup is fixed in the vibration free table. The holder for piezoelectric bimorph cantilevers is connected to a micrometer stand that is used to tune the distance between the free end of piezoelectric cantilever and the plectrum edge on the rotary cylinder. The position between the plectrum and piezoelectric bimorph will affect the maximum tip displacement of the piezoelectric bimorph cantilever. Electric motor is connected to the rotary cylinder. The pulsed force generated by the motor is a tunable factor during measurements.

The piezoelectric transducers used in this research are the QuickPack piezoelectric transducers bought from MIDE Company (Figure 3.1-4). The outside dimensions of every individual bimorph were $41.40 \times 17.02 \times 0.76 \text{ mm}^3$. The QuickPack piezoelectric transducers are robust, easy to be connected, hermetically sealed with increased life-time. The size is also suitable for small scale energy harvesters.



Figure 3.1-4 QuickPack piezoelectric bimorph cantilever (QP21 from MIDE Company)

The parameters of the material properties are listed in Table 3.1-1. For a given material with a certain dimension, the generated electrical power under a certain force F is (Priya, 2005):

$$P = \frac{1}{2} \frac{d^2}{\epsilon_0 \epsilon^x} \cdot F^2 \cdot \frac{t}{A} \cdot f = \frac{1}{2} (d \cdot g) \cdot F^2 \cdot \frac{t}{A} \cdot f \quad (3.1-1)$$

According to Equation (3.1-1), under certain experimental conditions (F, f), for a given material of fixed area A and thickness t , the electrical power is dependent on the $d \cdot g$ value of the piezoelectric material. Frequency f is the reciprocal of the time interval between every two impacts. For E-REH, this frequency is equal to the rotational frequency. It is better to choose high product of $d \cdot g$ value for PEH device. Besides the material properties, the output voltage V and f are two important factors in power output. Table 3.1-1 gives the piezoelectric constants of the piezoelectric material.

The piezoelectric bimorph is working in parallel mode. Figure 3.1-5 shows the schematic diagram of the experiment. In experiment, the electrical part is a resistive load connected directly to the piezoelectric output ends. The output voltage across the resistive load is recorded and analyzed by Oscilloscope (Portable FFT Analyzer CF-3400) and PC. The average output power will be obtained and shown in the next section under various input conditions.

Table 3.1-1 Piezoelectric constants of the ceramics (CTS-3195HD)

Parameters	Values
d_{31} (10^{-12} m/V or C/N)	-190
d_{33} (10^{-12} m/V or C/N)	390
g_{31} (10^{-3} Vm/N)	-11.3
g_{33} (10^{-3} Vm/N)	24
$d_{31} * g_{31}$ (10^{-15} m ² /N)	2147
$d_{33} * g_{33}$ (10^{-15} m ² /N)	9360
Q_m	80

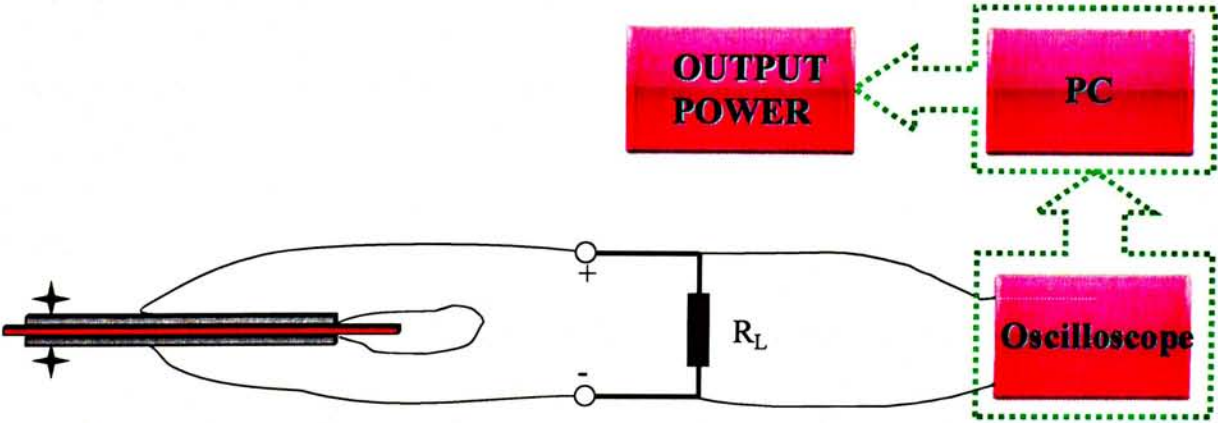


Figure 3.1-5 Schematic diagram of the experimental setup

3.2 *Output Power*

The power output of the piezoelectric extended rotary energy harvester is studied in this section. The output power will be calculated by the measured output voltage and current across a 15 k Ω resistive load. Different parameters are investigated on the power output.

3.2.1 *Maximum tip displacement on output power*

As shown in Figure 3.2-1, the plectrum begins to pluck the piezoelectric bimorph at point A. They will move together and separate at point B. The tip displacement at point B is the maximum tip displacement u_{max} during the impact process. u_{max} is decided by the distance d_{ol} between the plectrum and the tip of piezoelectric cantilever. d_{ol} is tuned by the movable micrometer stand. The external force should be equal or larger than the maximum restoring forces F_R due to the stiffness of the cantilever.

In the first part of experiments, we change the maximum tip displacement of the piezoelectric bimorph, which affects F_R during the impact process. We investigate the relationship between the output power and the maximum tip displacement. The piezoelectric bimorph cantilevers are fixed in parallel on a pedestal base. Meanwhile, a micrometer stand is connected with the base to tune the position of the piezoelectric cantilevers. The tunable overlap distance can be down to 0.02 mm.

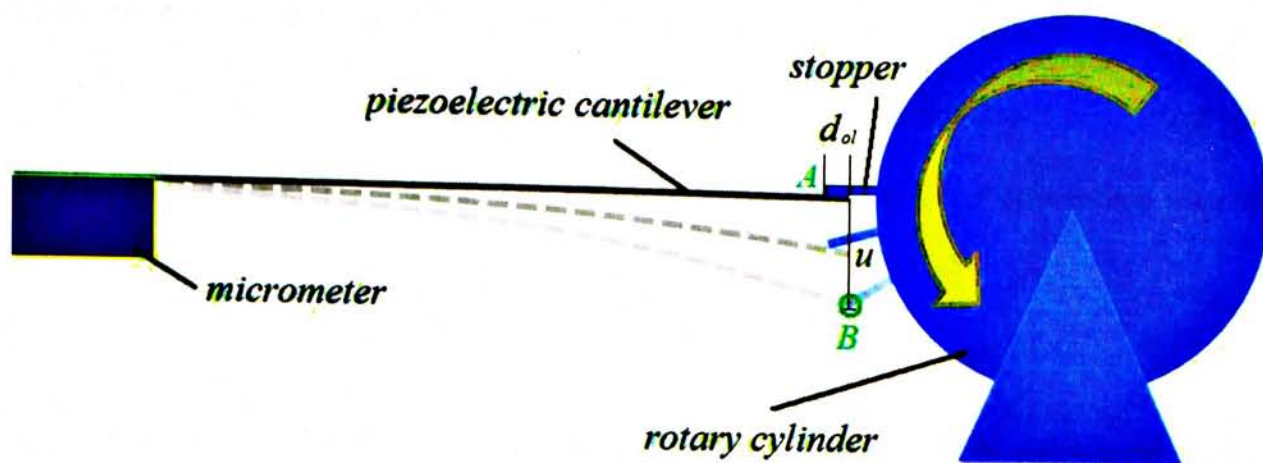


Figure 3.2-1 Schematic of the impact process

The vibration amplitude is related to the maximum tip displacement where the piezoelectric cantilever will separate from the plectrum. Therefore, the generated power is related to the maximum tip displacement of the piezoelectric cantilever.

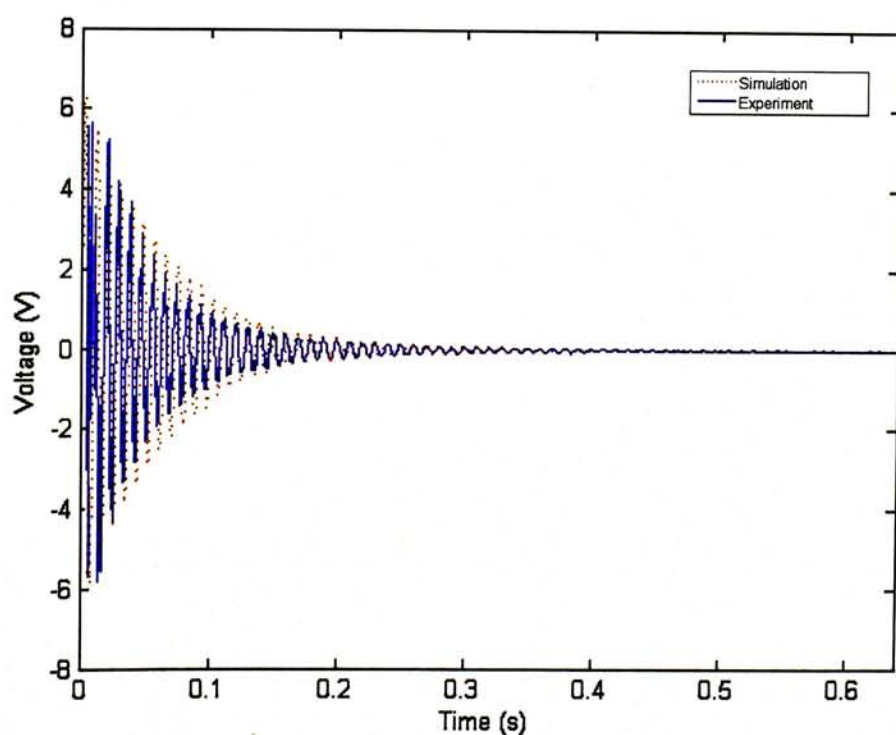


Figure 3.2-2 Time response of output voltage ($f = 1 \text{ Hz}$, $u_{\max} = 1.5 \text{ mm}$)

Experiments are carried out to investigate the output voltage and output power. Figure 3.2-2 shows the output voltage when the maximum tip displacement is 1.5 mm and rotational frequency is $f=1$ Hz. The simulation results are in good agreement with the experimental data.

The output power under different maximum tip displacement is calculated by ten pieces of piezoelectric cantilevers. As discussed above, the maximum tip displacement will affect the voltage generated by the piezoelectric bimorph. Figure 3.2-3 is the output power versus maximum tip displacement. The square markers are the experimental data with increasing maximum tip displacement. The red dot line represents the corresponding simulation results. It can be seen from this figure that, the larger of the maximum tip displacement, the larger power generated by the piezoelectric cantilevers. The simulation results are in good agreement with the experimental data.

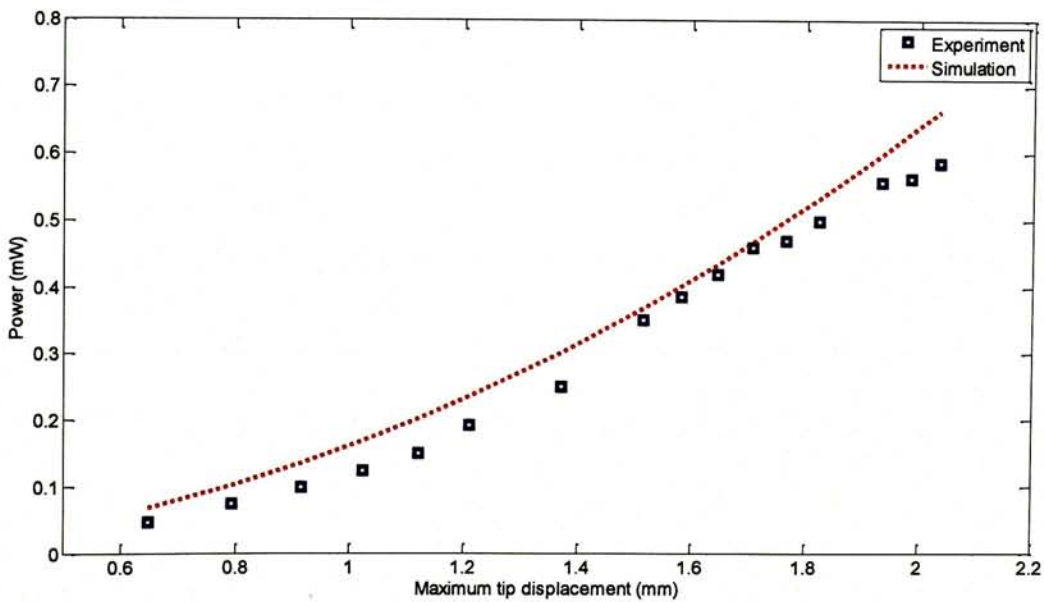


Figure 3.2-3 Output power versus maximum tip displacement ($f=0.78$ Hz)

3.2.2 Rotational frequency on output power

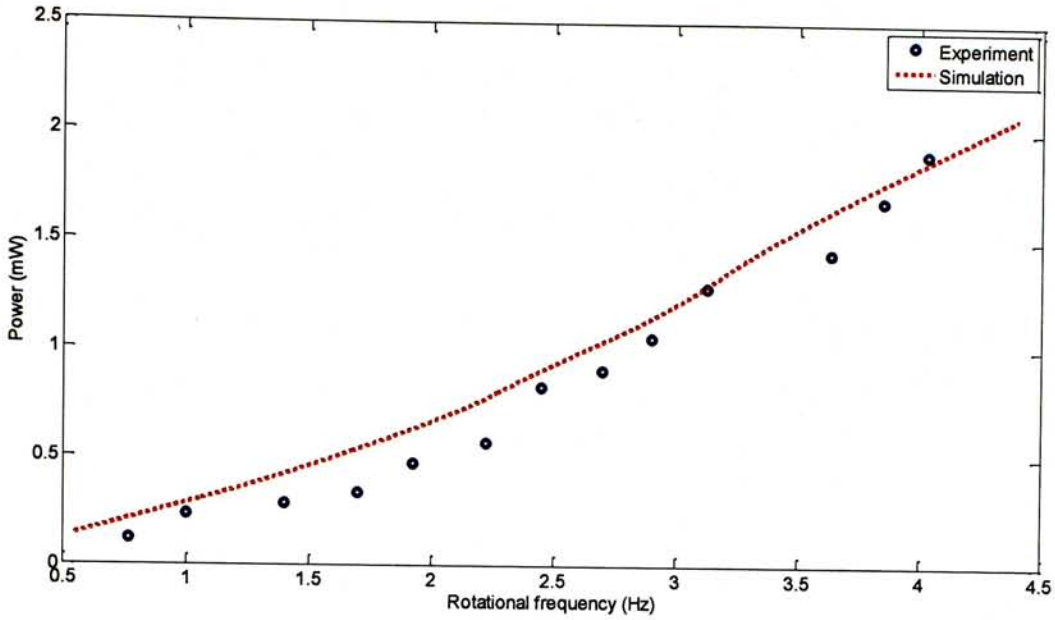


Figure 3.2-4 Average output power versus rotational frequency ($u_{\max} = 1.5$ mm)

The experiments under the changing rotational frequency condition are conducted in this section. In this part, the maximum tip displacement is kept to be constant $u_{\max} = 1.5$ mm. The power output is evaluated by changing the rotational frequency from low to high. Figure 3.2-4 shows the experimental results together with the simulation results of the power output versus rotational frequency.

The circular markers are the experimental data with increasing rotational frequency. The red dot line represents the corresponding simulation results. It can be seen from this figure that, the output power increases with the rotational frequency.

The cantilever is deflected by the plucking motion of the plectrum under a given displacement after which is expected to be released. After releasing, the piezoelectric cantilever will start to vibrate with no interaction with the plectrum. It can be

understood that the piezoelectric cantilever vibrates after an input pulse as if an initial quantity of mechanical energy had been injected into it. The mechanical energy mainly exists in elastic potential energy that is $E_e = \frac{1}{2} K_E u_{\max}^2$. Then the energy harvesting efficiency is the ratio of E_h / E_e , where E_h is the energy harvested from the vibrating piezoelectric cantilever. When $u_{\max} = 1.5$ mm, $f = 1$ Hz, $E_h = 0.248$ mJ, then the energy harvesting efficiency is 2.4%.

For the purpose of applications, the amount of electricity was usually considered to evaluate the performance of the devices. On the other hand, researchers have also conducted investigation on power efficiency by improving the design, harvesting circuitry and power storage devices ([Ng and Liao, 2005](#); [Wu et al. 2006](#)). Priya (2005) optimized the output power of piezoelectric windmill by choosing the matching load resistance in the device. He indicated that the matching load was equal to the internal resistance of the piezoelectric structure. In our case, the internal resistance is estimated by the equivalent circuit shown in Figure 2.2-3 and expressed as:

$$R_{in} = \frac{1}{\left(\frac{1}{j\omega L_1 + R_1 + \frac{1}{j\omega C_1}} + j\omega C_0 \right)} \quad (3.2-1)$$

Table 3.2-1 Parameters in equivalent circuit

Parameter	Value
R_1	504.586 k Ω
L_1	33.44 kH
C_1	71 pF
C_0	15.49 nF

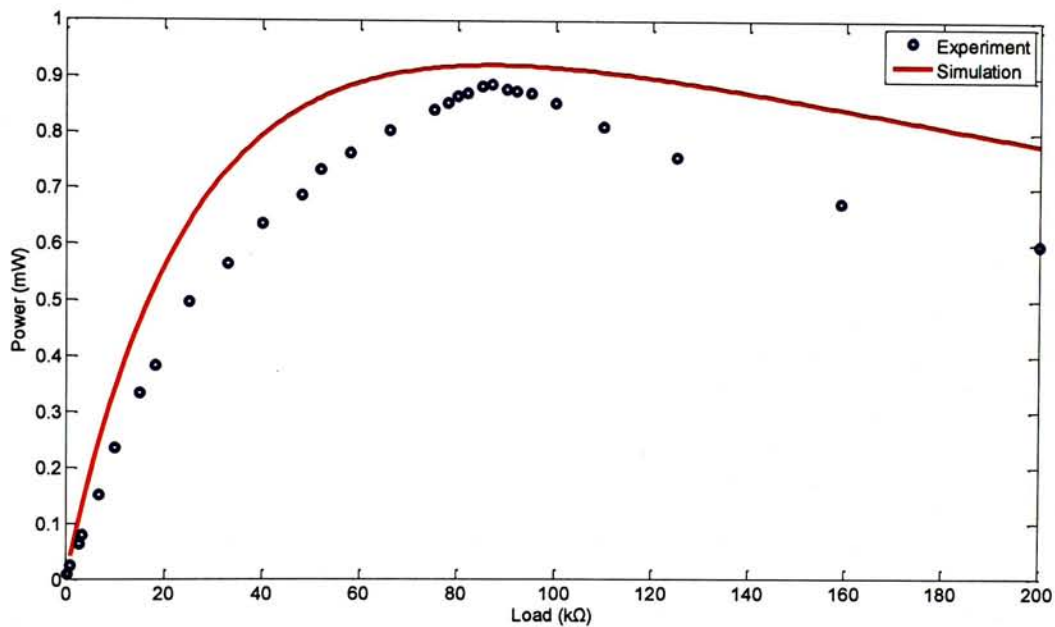


Figure 3.2-5 Average power output versus load resistance ($\mu_{\max} = 1.5$ mm, $f = 1.25$ Hz)

Parameters are measured by Impedance Analyzer (HP 4294) and given in Table 3.2-1. By using these parameters, the internal resistance R_{in} is calculated as 87 k Ω . Power output with varying load resistance are tested and shown in Figure 3.2-5. The analytical result is in agreement with the experimental data. Using load resistance $R = 85$ k Ω , harvesting efficiency reaches 6.9 % under 1.25 Hz rotational frequency.

3.3 Chapter Summary

A prototype of E-REH was fabricated and tested. The experimental setup was provided. Power output performances with different maximum tip displacement of the piezoelectric bimorph cantilever and varying rotational frequency were evaluated. The developed model was validated experimentally. The results showed that the output power increases with maximum tip displacement and rotational frequency.

CHAPTER FOUR COMPARISON BETWEEN E-REH AND REH

One original design of rotary structure for energy harvesting is to arrange piezoelectric bimorph transducers along the circumference. This structure is represented by the piezoelectric windmill (Priya et al., 2005). Priya (2005) has developed the analytical modeling for this piezoelectric windmill. 12 pieces of piezoelectric bimorphs were used in the fabricated prototype.

As discussed in Chapter Two, we proposed an extended rotary energy harvester (E-REH) with specific arrangement of plectra. E-REH and REH could have different performances under various input conditions. Comparison on their output power will be made.

4.1 Force on Output Power

Our energy harvester is designed for the rotary condition. The rotary motion can drive the device to transfer mechanical energy into electrical energy.

By using the model developed in Chapter Two, the power simulation results by ten pieces of piezoelectric bimorphs for both E-REH and REH can be obtained. Figure 4.1-1 shows the results under varying input force while the rotational frequency is kept constant.

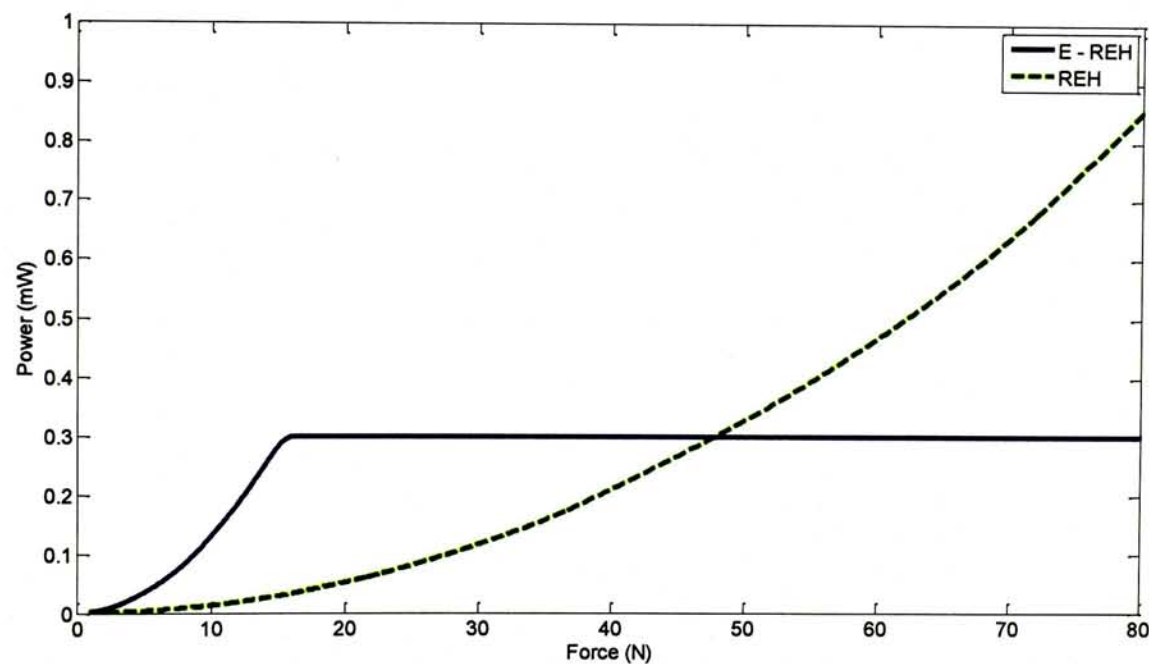


Figure 4.1-1 Power output comparison between E-REH and REH under input pulse with varying force amplitude ($f=1\text{ Hz}$)

As shown in Figure 4.1-1, the power generated by the REH increases with the input force amplitude. For the E-REH, the power also increases with the force before the critical point beyond which the power keeps constant. As discussed in Chapter Three, the force borne by the piezoelectric bimorph is affected by the maximum tip displacement. In E-REH structure, the force is applied on each piezoelectric cantilever. Therefore, there is a limit on force that is allowed to be applied on the piezoelectric cantilever. When the force is larger than this maximum force, the output power will be saturated. E-REH has higher output power than REH in relatively lower range of force. However, the REH can forereach E-REH by increasing the force.

In E-REH, the critical point of force is the restoring force due to the stiffness of the structure at the maximum tip displacement. This critical point is mainly affected by two factors: total structure stiffness K_E and maximum tip displacement. Results are shown in Figure 4.1-2. The critical force increases proportionally with the product of the total stiffness and maximum tip displacement of the piezoelectric cantilever.

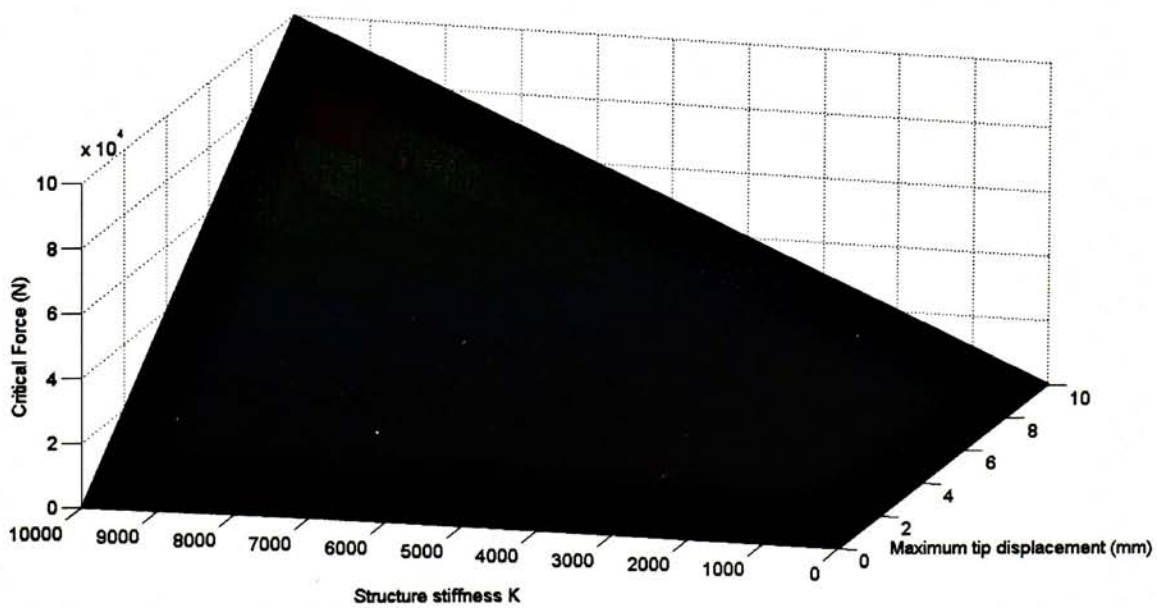


Figure 4.1-2 Critical force versus total stiffness and maximum tip displacement

4.2 Rotational Frequency on Output Power

We can also compare the output power of these two kinds of structures under different rotational frequencies. Before the comparison, the output voltage with increasing rotational frequency will be discussed. In REH structure, when the rotational frequency is f_0 , the impact frequency which is the reciprocal of the time interval between every two impacts on each piezoelectric cantilever will be $n \times f_0$.

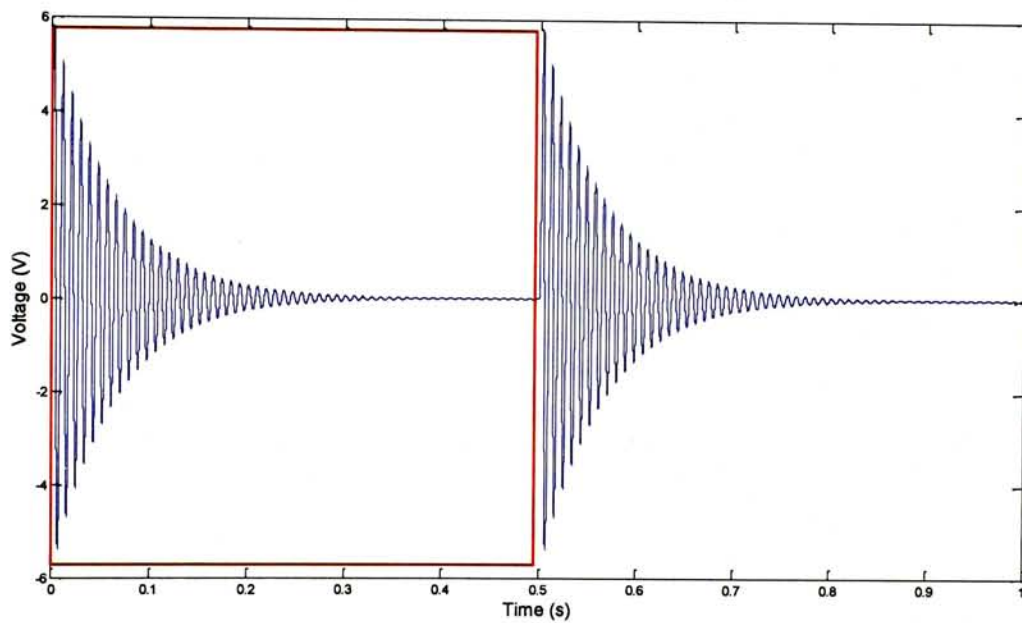


Figure 4.2-1 Time response of output voltage by one piezoelectric cantilever in REH ($f = 0.2$ Hz)

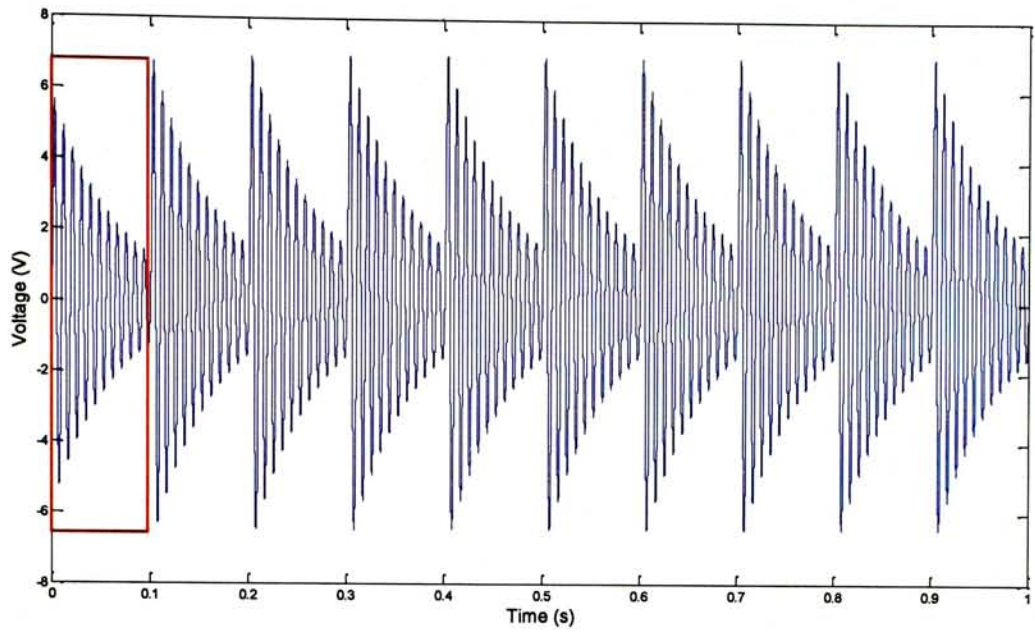


Figure 4.2-2 Time response of output voltage by one piezoelectric cantilever in REH ($f = 1$ Hz)

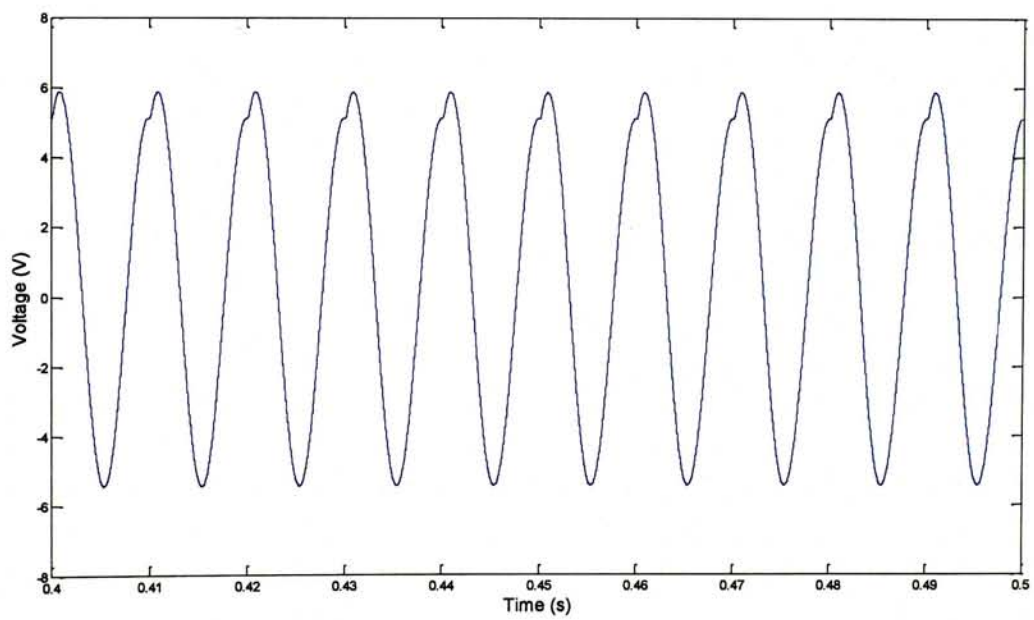


Figure 4.2-3 Time response of output voltage by one piezoelectric cantilever in REH ($f = 10$ Hz)

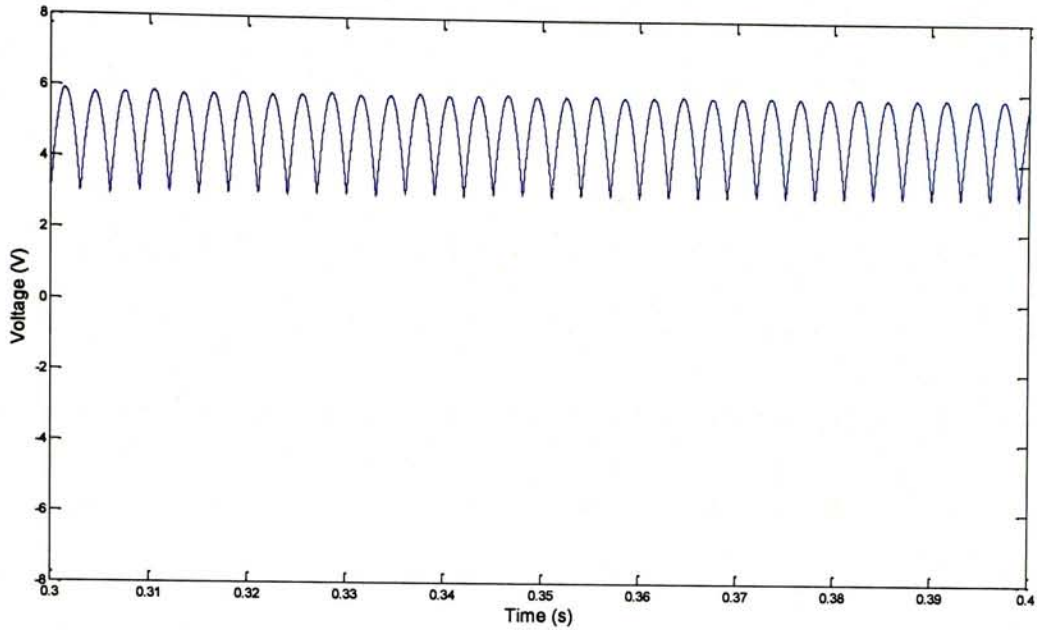


Figure 4.2-4 Time response of output voltage by one piezoelectric cantilever in REH ($f = 13$ Hz)

The time response of voltage under 0.2 Hz input rotational frequency is shown in Figure 4.2-1. The cantilever is deflected by the plucking motion of the plectrum under a given displacement after which is expected to be released. Then the cantilever will vibrate freely. The vibration amplitude decreases to near zero after 0.5 s because of the damping. The vibration response by one pluck is marked by the red box. Suppose the total energy generated by the vibrations within the red box is E_0 . Then the total energy accumulated in 1 second is $2E_0$. However, when increasing the input rotational frequency, the number of vibrations by plucks within a certain time interval (e.g., 1 second) will increase but the vibration by one pluck would be stopped by the next pluck. In this case, the energy generated by each incomplete vibration (without decaying to zero) corresponding to each pluck will be smaller than E_0 . For example, total energy accumulated by 1 Hz input rotational frequency within 1 second is smaller than $10E_0$ (see Figure 4.2-2). Nevertheless, the total energy could still

increase with the input rotational frequency. But the increasing gradient of output power with increasing input rotational frequency will be slowed down.

The first nature frequency of the piezoelectric cantilever in this research is near 100 Hz. Therefore, if the rotational frequency is 10 Hz (see Figure 4.2-3) then the impact frequency on one piezoelectric cantilever in REH is 100 Hz. That means the cantilever will be plucked to the maximum displacement and vibrate for one cycle (~ 0.01 s) before being forced to restart the next cycle by the next coming impact. The vibration amplitude will approximately be kept as the maximum tip displacement. Beyond 10 Hz input rotational frequency, the cantilever in REH could not vibrate for one complete cycle or even cannot vibrate in high frequency range. Figure 4.2-4 shows the voltage output under the rotational frequency of 13 Hz. The amplitude is obviously smaller as compared with Figure 4.2-3. Therefore, the output power will be decreased with rotational frequency beyond 10 Hz. However, this peak frequency is postponed to higher range for E-REH structure. The comparison results between E-REH and REH are shown in Figure 4.2-5.

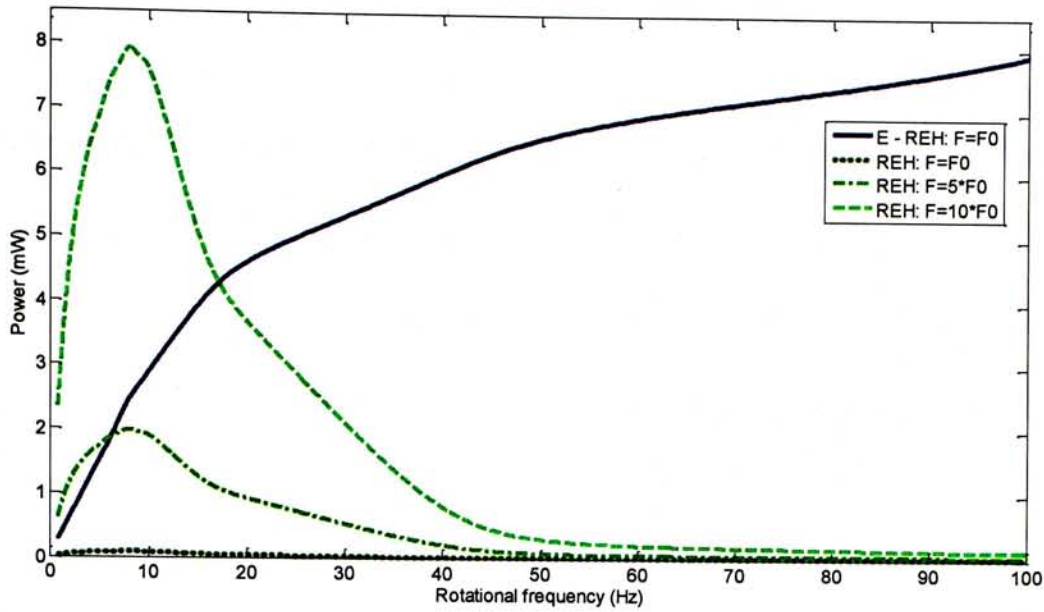


Figure 4.2-5 Comparison on output power between E-REH and REH with varying rotational frequency

The E-REH has higher output power than REH when the input forces are same for both designs. Particularly, in higher rotational frequencies, power output of E-REH still increases with rotational frequency but the REH structure has shown downtrend after 10 Hz. The downtrend of the E-REH is shifted to high frequency. Therefore, in lower frequency range, the REH can have higher power output by increasing force input into its structure. However, the E-REH will have higher output power performance in higher rotational frequency range even the applied force to the harvester is smaller than that applied to the REH.

4.3 Comparison on Design Space

Considering both rotational frequency and force amplitude, their power output is compared between the E-REH and REH. Figures 4.3-1 and 4.3-2 respectively show the power performances by ten piezoelectric cantilevers of both E-REH and REH varying with both factors discussed in the previous two subsections. Figure 4.3-3 shows both E-REH and REH cases for the purpose of comparison. Observing this diagram, it will be convenient for us to identify the useful region between these two designs. The REH has higher output power in larger force with lower rotational frequency condition. And the E-REH has higher output power in the low force, low rotational frequency condition. In high rotational frequency range, the E-REH has higher output power than the REH. As shown in the figure, the range that the E-REH outperforms the REH is much broader.

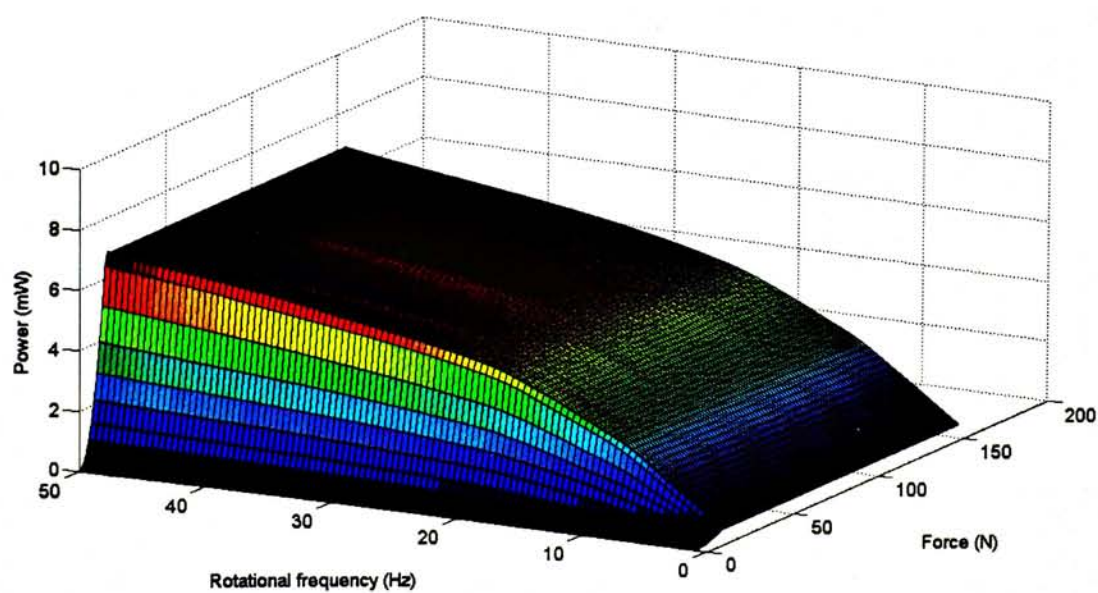


Figure 4.3-1 Variation of the output power by E-REH under different impact force and rotational frequency

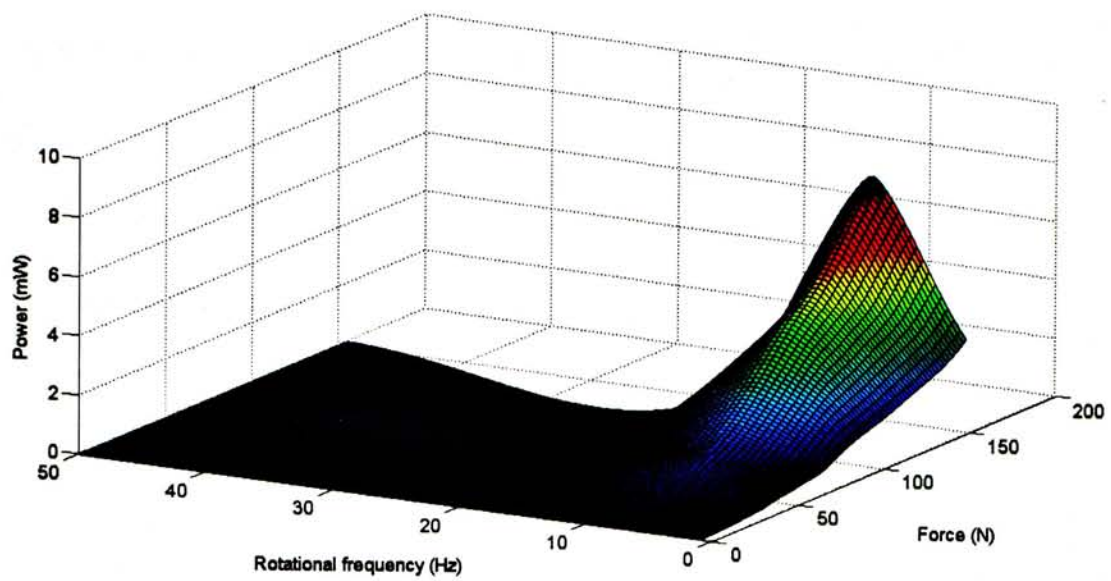


Figure 4.3-2 Variation of the output power by REH under different impact force and rotational frequency

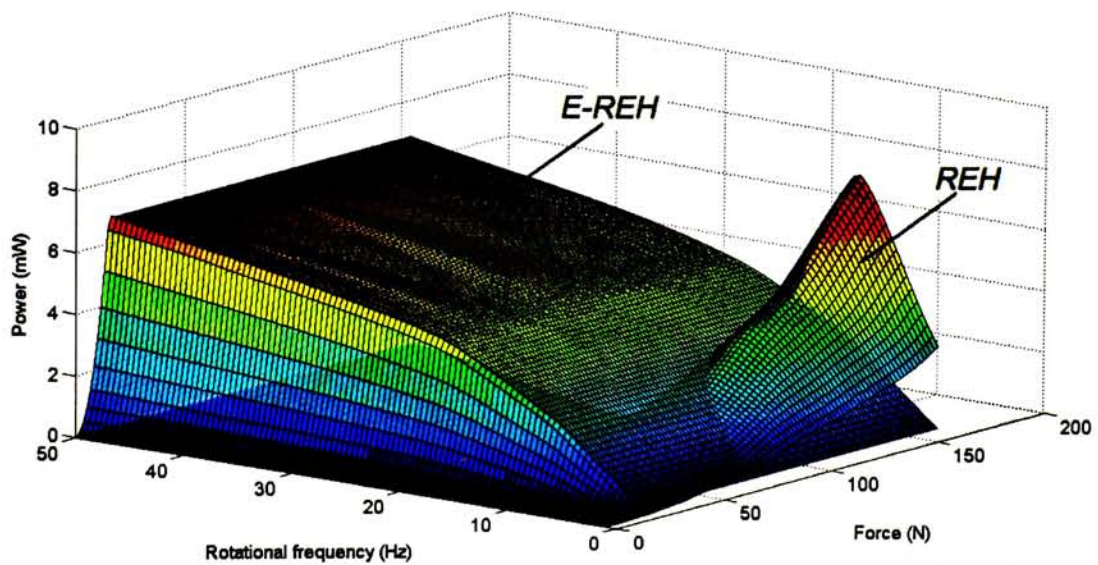


Figure 4.3-3 Variations of the output power by both E-REH and REH under different impact force and rotational frequency

The E-REH design has broader effective range for output power as compared to the REH. Thus, the E-REH would be more suitable for energy harvesting from windmills or other fan structures with higher rotating speed. In addition, the E-REH would also be suitable for energy harvesting from rotations with relatively lower force and rotational frequency: rotary entrance doors, turnstiles in ticket gates in the subway stations and turnstile entrance gates in supermarkets or parks.

4.4 Chapter Summary

Comparisons on power output between REH and E-REH were made in this chapter.

The comparison results showed:

1. In large force but low rotational frequency condition: both designs could be utilized, but REH has higher output power than E-REH;
2. In relatively lower force and lower rotational frequency condition: E-REH has higher output power;
3. In high rotational frequency condition, E-REH outperforms REH in terms of output power; REH may be working ineffectively in high rotational frequency condition;
4. The effective energy harvesting range of E-REH could be much broader as compared to REH.

These results could help us utilize both designs under suitable working conditions.

CHAPTER FIVE CONCLUSION AND FUTURE WORK

5.1 *Conclusion*

In this research, an extended rotary energy harvester (E-REH) was proposed. The piezoelectric E-REH that can scavenge energy from rotational motion was designed. New features were discussed as compared to the rotary energy harvester (REH). Model of the impact-based piezoelectric energy harvester was developed. The prototype was fabricated and tested. Model was validated by the experimental results and used to analyze the output power performances of the E-REH and REH, respectively. Working range was also discussed.

The contributions of this thesis include:

1. Principle and design of an extended rotary energy harvester that can scavenge rotary motion energy were given;
2. Power performances of the E-REH under different conditions were studied;
3. Working ranges for both E-REH and REH were compared and discussed.

The size of piezoelectric material affects the output power generated by the device. Using the materials with the dimensions in our prototype, the E-REH can provide power of several milliwatts. REH has higher output power under large force but low rotational frequency condition. E-REH has higher output power under low force and low rotational frequency condition. In high rotational frequency condition, E-REH outperforms REH. These results could help us utilize both designs under suitable working conditions.

5.2 *Future Work*

A prototype of the E-REH was fabricated and tested. Since the ultimate goal is to harvest energy from ambient sources, the next step is to apply the E-REH in various applications. The devices need to be optimized for specific working conditions in order to provide better output power performances.

Harvesting circuit and energy storage devices are needed to accumulate the energy for intermittent use. In this thesis, the output power was measured by a resistive load that was directly connected to the piezoelectric element. This method was widely used in the PEH development. Existing researches concerned with the harvesting circuits and storage devices were mostly for energy harvesting under harmonic excitations. In the future, impact-based energy harvesting circuits and storage devices should be investigated.

BIBLIOGRAPHY

Abramovich, H. 2009, "Power harvesting from apparatus, system and method," *US Patent*, 2009/0195226 A1, Aug. 6, 2009.

Ackermann, T. and Soder, L. 2000, "Wind energy technology and current status: a review," *Renewable and Sustainable Energy Reviews*, **4**, 315-74.

Ajitsaria, J., Choe, S. Y., Shen, D., and Kim, D. J. 2007, "Modeling and analysis of a bimorph piezoelectric cantilever beam for voltage generation," *Smart Materials and Structures*, **16**(2), 447.

Anton, S. R., and Sodano, H. A. 2007, "A Review of Power Harvesting using Piezoelectric Materials (2003-2006)," *Smart Materials and Structures*, **16**, R1-R21.

Badel, A., Guyomar, D., Lefeuvre, E., and Richard, C. 2005, "Efficiency enhancement of a piezoelectric energy harvesting device in pulsed operation by synchronous charge inversion," *Journal of Intelligent Material Systems and Structures*, **16**(10), 889-901.

Beeby, S. P., Tudor, M. J., and White, N. M. 2006, "Energy harvesting vibration sources for Microsystems applications," *Measurement Science and Technology*, **17**(12), R175-195.

Bogue, R. 2009, "Energy harvesting and wireless sensors: a review of recent

developments,” *Sensor Review*, **29**(3), 194-199.

Cook-Chennault, K. A., Thambi, N., and Sastry, A. M. 2008, “Powering MEMS portable devices — a review of non-regenerative and regenerative power supply systems with special emphasis on piezoelectric energy harvesting systems,” *Smart Materials and Structures*, **17**(4), 043001 (33pp).

Donelan, J. M., Li, Q., Naing, V., Hoffer, J. A., Weber, D. J., and Kuo, A. D. 2008, “Biomechanical energy harvesting: generating electricity during walking with minimal user effort,” *Science*, **319**(5864), pp. 807–810.

Fang, H. B., Liu, J. Q., Xu, Z. Y., Dong, L. U., Wang, L., Chen, D., Cai, B. C., and Liu, Y. 2006, “Fabrication and performance of MEMS-based piezoelectric power generator for vibration energy harvesting,” *Microelectronic Journal*, **37**, 1280-4.

Gautschi, G. 2002, “Piezoelectric sensorics: force, strain, pressure, acceleration and acoustic emission sensors,” *Materials and Amplifiers*, Springer.

Gilbert, J. and Balouchi, F. 2008, “Comparison of energy harvesting systems for wireless sensor networks,” *International Journal of Automation and Computing*, **5**(4), 334-347.

Gu, L. and Livermore, C. 2011, “Impact-driven, frequency up-converting coupled vibration energy harvesting device for low frequency operation,” *Smart Materials and Structures*, **20**(2011), 045004 (10pp).

Guan, M. J. and Liao, W. H. 2007, "On the efficiencies of piezoelectric energy harvesting circuits towards storage device voltages," *Smart Materials and Structures*, **16**(2), 498-505.

Guan, M. J. and Liao, W. H. 2008, "Characteristics of energy storage devices in piezoelectric energy harvesting systems," *Journal of Intelligent Material Systmes and Structures*, **19**(6), 671-680.

Huang, C., Lin, Y. Y., and Tang, T. A. 2004, "Study on the tip-deflection of a piezoelectric bimorph cantilever in the static state," *Journal of Micromechanics and Microengineering*, **14**, 530-34.

Hudak, N. S. and Amatucci, G. G. 2008, "Small-scale energy harvesting through thermoelectric, vibration, and radiofrequency power conversion," *Journal of Applied Physics*, **103**(10), 101301.

IEEE Standard on Piezoelectricity 1988, *ANSI/IEEE Std.*, 176-1987.

Jia, D. and Liu, J. 2009, "Human power-based energy harvesting strategies for mobile electronic devices," *Front. Energy Power Eng. Chin.*, **3**(1), 27-46.

Khaligh, A., Zeng, P., and Zheng, C. 2010, "Kinetic energy harvesting using piezoelectric and electromagnetic technologies—State of the art," *Proceedings of IEEE Transactions of Industrial Electronics.*, **57**, No. 3.

Kulah, H. and Najafi, K. 2004, "An electromagnetic micro power generator for low-frequency environmental vibrations," *Proceedings of 17th IEEE Int. Conf. on Micro Electro Mechanical Systems*, pp. 237-40.

Kymissis, J., Kendall, C., Paradiso, J., and Gershenfeld, N. 1998, "Parasitic power harvesting in shoes," *Proceedings of Second International Symposium on Wearable Computers*, pp. 132-139.

Kyono, T., Suzuki, R. O., and Ono, K. 2003, "Conversion of unused heat energy to electricity by means of thermoelectric generation in condenser," *Proceedings of IEEE Trans. Energy Convers.*, **18**, 330-4.

Leurial, J. P., Snyder, G. J., Patel, J., Huang, C. K., Ryan, M. A., Averbach, R., Hill, C., and Chen, G. 2001, "Solid-state power generation and cooling micro/nanodevices for distributed system architectures," *Proceedings of International Conference on Thermoelectric Energy Conversion, (8-11 June 2001)*, pp. 24-9.

Liang, J. R. and Liao, W. H. 2009, "Piezoelectric energy harvesting and dissipation on structural damping," *Journal of Intelligent Material Systems and Structures*, **20**, No. 5, pp. 515-527.

Liang, J. R. and Liao, W. H. 2010, "Impedance matching for improving piezoelectric energy harvesting systems," *Proceedings of SPIE Conference on Smart Structures and Materials: Active and Passive Smart Structures and Integrated Systems 2010*,

SPIE Vol. **7643**, 76430K (12 pages); doi:10.1117/12.847524.

Liang, J. R. and Liao, W. H. 2011, "Energy flow in piezoelectric energy harvesting systems," *Smart Materials and Structures*, **20**, 015005, 2011, DOI:10.1088/0964-1726/20/1/015005.

Mateu, L. and Moll, F. 2005, "Review of energy harvesting techniques and applications for microelectronics," *Proceedings of SPIE*, **5837**(1), 359-373.

Mathuna, C. O., O' Donnell, T., Martinez-Catala, R. V., Rohan, J., and O' Flynn, B. 2008, "Energy scavenging for long-term deployable wireless sensor networks," *Talanta*, **75**(3), 613-623.

Millikena, C., Guruswamy, S., and Khandkarb, S. 1999, "Degradation of some ceria electrolytes under hydrogen contact nearby anode in solid oxide fuel cells (SOFCs)," *Journal of The Electrochemical Society*, **146**, 872-82.

Mitcheson, P. D., Yeatman, E. M., Rao, G. K., Holmes, A. S., and Green, T. C. 2008, "Energy harvesting from human and machine motion for wireless electronic devices," *Proceedings of IEEE*, **96**(9), 1457-1486.

Ng, T. H. and Liao, W. H. 2005, "Sensitivity analysis and energy harvesting for a self-powered piezoelectric sensor," *Journal of Intelligent Material Systems and Structures*, **16**, No. 10, pp. 785-97, 2005.

Op het Veld, B., Hohlfeld, D., and Pop, V. 2009, "Harvesting mechanical energy for ambient intelligent devices," *Information Systems Frontiers*, **11**(1), 7-18.

Ottman, G., Hofmann, H., Bhatt, A. And Lesieutre, G. A., L. 2002, "Adaptive piezoelectric energy harvesting circuit for wireless remote power supply," *Proceedings of IEEE Transactions on Power Electronics*, **17**(5), 669-76.

Ottman, G., Hofmann, H. and Lesieutre, G. A., L. 2003, "Optimized piezoelectric energy harvesting circuit using step-down converter in discontinuous conduction mode," *Proceedings of IEEE Transactions on Power Electronics*, **18**(2), 696-703.

Paradiso, J. A. and Feldmeier, M. 2001, "A compact, wireless, self-powered pushbutton controller," *UbiComp 2001: Ubiquitous Computing, ACM UBICOMP Conference Proceedings*, Springer-Verlag Berlin Heidelberg, pp. 299–304.

Paradiso, J. A. and Starner, T. 2005, "Energy scavenging for mobile and wireless electronics," *IEEE Pervasive Computing Magazine*, **4**(1), 18-27.

Priya, S., Chen C. T., Fye D. and Zahnd J. 2005, "Piezoelectric windmill: a novel solution to remote sensing," *Japanese Journal of Applied Physics*, **44**, No. 3, pp. L104-L107, 2005.

Priya, S. 2005, "Modeling of electric energy harvesting using piezoelectric windmill," *Applied Physics Letters*, **87**, 184191.

- Priya, S. 2007, "Advances in energy harvesting using low profile piezoelectric transducers," *Journal of Electroceramics*, **19**, 165–182.
- Regan, B. O. and Gratzel, M. 1991, "A low-cost, high-efficiency solar cell based on dye-sensitized colloidal TiO₂ films," *Nature*, **353**, 737-40.
- Renaud, M., Fiorini, P., and van Hoof, C. 2007, "Optimization of a piezoelectric unimorph for shock and impact energy harvesting," *Smart Materials and Structures*, **16**(4), 1125-1135.
- Renaud, M., Fiorini, P., Schaijk, R. van, and van Hoof, C. 2009, "Harvesting energy from the motion of human limbs: the design and analysis of an impact-based piezoelectric generator," *Smart Materials and Structures*, **18**, 035001 (16pp)
- Rodig, T., Schonecker, A., and Gerlach, G. 2010, "A survey on piezoelectric ceramics for generator applications," *Journal of the American Ceramic Society*, **93**(4), 901-912.
- Roundy, S., Wright, P. K., and Rabaey, J. 2003, "A study of low level vibrations as a power source for wireless sensor nodes," *Computer Communications*, **26**, 1131-44.
- Sakakibara, T., Izua, H., Shibata, T., Tarui, H., Shibata, K., Kiyama, S., and Kawahara, N. 2002, "Multi-source power supply system using micro-photovoltaic devices combined with microwave antenna," *Sensors Actuators*, **95**, 208-11.

Shenck, N. and Paradiso, J. 2001, "Energy scavenging with shoe-mounted piezoelectrics," *Proceedings of IEEE Micro*, **21**(3), 30-42.

Skoog, D. A., Holler, F. J., and Crouch, S. R. 2007, "Chapter 1", *Principles of Instrumental Analysis (6th ed.)*, Cengage Learning, pp.9, ISBN: 9780495012016.

Smits, J. G. and Choi, W. S. 1991, "The constituent equations of piezoelectric heterogeneous bimorphs," *Proceedings of IEEE Transactions on Ultrasonics, Ferroelectrics, and Frequency Control*, **38**, No. 3.

Sodano, H, Inman, D. J., and Park, G. 2004, "A review of power harvesting from vibration using piezoelectric materials," *Shock and Vibration Digest*, **36**, 197–205.

Sodano, H. A., Inman, D. J. and Park, G. 2005a, "Comparison of piezoelectric energy harvesting devices for recharging batteries," *Journal of Intelligent Material Systems and Structures*, **16**(10), 799-807.

Sodano, H. A., Inman, D. J. and Park, G. 2005b, "Generation and storage of electricity from power harvesting devices," *Journal of Intelligent Material Systems and Structures*, **16**(1), 67-75.

Stronge, W. J. 2000, *Impact Mechanics* (Cambridge: Cambridge University Press), pp.3.

Tan, Y. K., Hoe, K. Y., and Panda, S. K. 2006, "Energy harvesting using piezoelectric

igniter for self-powered radio frequency (RF) wireless sensors,” *Proceedings of IEEE International Conference on Industrial Technology 2006*, pp. 1711-1716.

Vainer, E. A. 1976, “Piezoelectric lighter,” *US Patent*, 3,947,731, Mar. 30, 1976.

Umeda, M., Nakamura, K., and Ueha, S. 1996, “Analysis of transformation of mechanical impact energy to electrical energy using a piezoelectric vibrator,” *Japanese Journal of Applied Physics*, **35**, 3267–73.

Umeda, M., Nakamura, K., and Ueha, S. 1997, “Energy storage characteristics of a piezo-generator using impact induced vibration,” *Japanese Journal of Applied Physics*, **36**, (part 1, No. 5B), 3146–3151.

Umeda, M., Sakai, Y., and Nakamura, K. 2003, “Self-generation door alarm system using impact induced piezoelectric vibration,” *Proceedings of IEEE. Transactions on Sensors and Micromachines*, **12**, 534–40.

Wacharasindhu, T. and Kwon, J.W. 2008, “A micromachined energy harvester from a keyboard using combined electromagnetic and piezoelectric conversion,” *Journal of Micromechanics and Microengineering*, **18**, 104016.

Wang, Q. M. and Cross, L. E. 1999, “Constitutive equations of symmetrical triple layer piezoelectric benders,” *IEEE Transactions of Ultrasonics, Ferroelectronics, and Frequency Control*, **46**, No. 6, 1343-51.

Wikipedia http://en.wikipedia.org/wiki/Energy_harvesting.

Wu, W. J., Chen, Y. F., Wang, C. S., and Chen, Y. H. 2006, "Smart wireless sensor network powered by random ambient vibrations, " *Proceedings of IEEE International Conference on Systems, Man, and Sybernetics*, Oct. 8-11, 2006.

Wu, W. J., Wickenheiser, A. M., Reissman, T., Garcia, E. 2009, "Modeling and experimental verification of synchronized discharging techniques for boosting power harvesting from piezoelectric transducers," *Smart Materials and Structures*, **18** (2009), 055012 (pp.14).

Xie, L., Menet, C. G., Ching, H., and Du, R. 2009, " The automatic winding device of a mechanical watch movement and its application in energy harvesting," *Journal of Mechanical Design*, **131**, Issue 7, 071005 (pp.7).

Yang, W. M., Chou, S. K., Shu, C., Xue, Li. Z. W., Li, D. T., and Pan, J. F. 2003, "Microscale combustion research for application to micro thermophotovoltaic systems," *Energy Conversion and Management*, **44**, 2625-34.

Yuen, S. C. L., Lee, J. M. H., Li, W. J., and Leong, P. H. W. 2007, "An AA-sized vibration-based microgenerator for wireless sensors," *IEEE Pervasive Computing Magazine*, **6**, 64-72.

CUHK Libraries



004777764